

# Structural basis for sirtuin 2 activity and modulation: Current state and opportunities

Received for publication, December 26, 2024, and in revised form, May 12, 2025. Published, Papers in Press, May 22, 2025.  
<https://doi.org/10.1016/j.jbc.2025.110274>

Samuel P. Bernhard<sup>1</sup>, Francesc X. Ruiz<sup>2</sup>, Stacy Remiszewski<sup>3</sup> , Matthew J. Todd<sup>3</sup>, Thomas Shenk<sup>3,4</sup> , John L. Kulp III<sup>1,3,\*</sup> , and Lillian W. Chiang<sup>3,\*</sup>

From the <sup>1</sup>Division of Chemistry, Conifer Point Pharmaceuticals, Doylestown, Pennsylvania, USA; <sup>2</sup>Chemistry and Chemical Biology, Center for Advanced Biotechnology and Medicine, Rutgers University, Piscataway, New Jersey, USA; <sup>3</sup>Evrys Bio Inc., Pennsylvania Biotechnology Center, Doylestown, Pennsylvania, USA; <sup>4</sup>Department of Molecular Biology, Princeton University, Princeton, New Jersey, USA

Reviewed by members of the JBC Editorial Board. Edited by Craig Cameron

Sirtuin 2 (SIRT2) is a ubiquitously expressed cellular enzyme that deacylates protein lysine residues using NAD<sup>+</sup> as a cofactor. SIRT2-mediated posttranslational modifications on a plethora of protein targets position the enzyme to exert a wide-ranging regulatory role in many physiological and pathological processes. More than 39 SIRT2 crystal structures in complex with substrates, products, mimetics of substrates and products, and modulators have been reported. The Rossmann fold of the catalytic core presents inducible acyl and cofactor-binding cavities that accommodate acyl chains of diverse lengths. These structures have provided information for the design of mechanism- and substrate-based inhibitors. Indeed, a specific SIRT2 selectivity pocket has been described and can be targeted by different chemotypes. Despite the determination of many crystal structures, numerous open questions remain, especially relating to the development of small molecule modulators, full or partial activation or inhibition, and relating these effects to different therapeutic applications. Additional questions include understanding the role of the disordered termini and the role of potential quaternary states (monomer, dimer, and trimer). Deeper insight into these issues may facilitate the development of SIRT2 selective modulators that can be tailored to different pathological scenarios, such as viral infections and cancers, in which either activation or inhibition of SIRT2 may be of therapeutic benefit. This review covers the following topics: (1) primary to quaternary and catalytic structural biology; (2) structural insights into molecular modulation of SIRT2 (inhibition and selectivity by mechanism-based inhibitors, substrate-mimicking inhibitors, C pocket-binding inhibitors, and selectivity pocket binding inhibitors, including insights to activation); and (3) the impact of structural variations (mutations, posttranslational modifications, polymorphs, protein interactions). Despite considerable progress, key knowledge gaps remain regarding the design of optimized SIRT2 modulators. Addressing these uncertainties, particularly within the realms of full/partial activation/

inhibition, off-target effects, and tailoring modulators to specific pathologies, will require further investigation into the roles of the SIRT2-disordered termini, quaternary states, and posttranslational modifications. Ultimately, unraveling these intricacies holds the key to unlocking the therapeutic potential of SIRT2 modulation.

Posttranslational acylation (*e.g.*, acetylation, myristoylation, *etc.*) of lysine residues is a key regulatory mechanism in eukaryotes (1, 2). The most thoroughly studied modification is lysine acetylation, which involves the transfer of an acetyl group from acetyl-CoA to the primary amine in the  $\epsilon$ -position of the lysine side chain within a protein, neutralizing the positively charged lysine. Hence, lysine acetyltransferases “write” marks, while lysine deacetylases (KDACs) “erase” them. A third group of proteins (*e.g.*, bromodomain-containing proteins) are the “readers,” that can recognize and bind acetylated lysines and trigger signal transduction cascades. The dynamic interplay between writers, erasers, and readers regulates critical cellular functions, namely epigenomic and metabolic processes (3).

KDACs are grouped by class based on sequence homology to the original yeast enzyme and are differentiated by sensitivity to trichostatin A inhibition (4). Sirtuins (SIRTs) are class III, NAD<sup>+</sup>-dependent KDACs that are insensitive to trichostatin A, differing from the class I and class II KDACs which are zinc dependent and inhibited by trichostatin A. SIRTs bind a zinc ion, but the zinc does not participate in the catalytic mechanism. The first-discovered SIRT was the *Saccharomyces cerevisiae* protein “silent information regulator 2” (Sir2), essential for the formation of silent heterochromatin (5). It was not until about a decade later that the role of Sir2 as key regulator of senescence was discovered (6). The discovery and study of SIRTs from all phyla have dramatically increased since that time. SIRTs comprise a large and ancient family of genes (7, 8).

The class III KDAC SIRT family is further organized into four phylogenetic classes based on their relationships to the yeast SIRTs, Sir2, the founding member, and additional yeast

\* For correspondence: authors: John L. Kulp III, [john.kulp@coniferpoint.com](mailto:john.kulp@coniferpoint.com); Lillian W. Chiang, [lillian@evrysbio.com](mailto:lillian@evrysbio.com).

SIRT2s, termed “homologs of sir two”, Hst1–4. For human SIRT2s, SIRT1, SIRT2, and SIRT3 belong to class I, SIRT4 to class II, SIRT5 to class III, and SIRT6 and SIRT7 to class IV. SIRT1 shares the highest sequence similarity with yeast Sir2 and Hst1, while SIRT2 and SIRT3 mimic Hst2. On the other hand, SIRT4 to SIRT7 are more closely related to prokaryotic, *D. melanogaster* and *C. elegans* SIRT2s (9–11). SIRT2s share an evolutionarily conserved catalytic core of ~250 amino acids, with N- and C-terminal domains of differing lengths and motifs (e.g., nuclear export signal, mitochondrial localization signal) that contribute to isoenzyme-specific localization and regulation. The seven members of the human SIRT2 family are ubiquitously expressed and play an important role in the regulation of metabolic pathways related to cell response to the environment, energy availability, and cellular stress. SIRT1, 6, and 7 are primarily nuclear, SIRT3, 4, and 5 are mitochondrial, and SIRT2 is primarily cytosolic. Their NAD<sup>+</sup> dependency and regulatory role in acetyl-CoA levels link their activity to the metabolic state of cells (12).

In this review, we are focusing on SIRT2 and on the current understanding of the structural basis for its catalysis and modulation. With regards to SIRT2 physiological and pathological roles in autoimmune, cancer, infection, neurologic and other disorders, we refer the reader to several comprehensive reviews (13–18).

### Structural basis for SIRT2 activity

The recent advent of AI-based protein structure prediction algorithms (19) can help visualize the intricate relationship of the different levels of protein structure, from primary to quaternary, and ultimately how they impact protein function. This section provides such a walkthrough for SIRT2.

#### Structure: primary to quaternary levels

##### Primary structure

The major SIRT2 isoform (Fig. 1A), designated 2.1, is comprised of 389 amino acids and features a disordered N terminus (amino acids 1–34) and C terminus (351–389). Amino acids 41 to 51 comprise a nuclear export signal (NES) motif that facilitates the movement of SIRT2 out of the nucleus and into the cytoplasm *via* the CRM1 export pathway (20). Conversely, the mechanism of SIRT2 nuclear import is uncertain, but recent proteomics data show that SIRT2 interacts with multiple nuclear importin proteins and that the C-terminus may act as a negative regulator of nuclear import by limiting importin–SIRT2 interactions (21). “Isoforms and polymorphisms” describes the different isoforms of SIRT2 in detail.

##### Secondary and tertiary structures

The structural basis for SIRT2 function has been reviewed in detail (22, 23). The termini of SIRT2 are mostly disordered as reflected in the recent computationally determined SIRT2

structure deposited in AlphaFold (<https://alphafold.ebi.ac.uk/entry/Q8IXJ6>, Fig. 1A). Most of the 39 crystal structures of human SIRT2 in the Protein Data Bank (PDB) have been determined using SIRT2 protein with truncated termini, typically containing amino acids 34 to 356 or 50 to 356 (see [https://www.rcsb.org/groups/sequence/polymer\\_entity/Q8IXJ6](https://www.rcsb.org/groups/sequence/polymer_entity/Q8IXJ6)). Two structures have captured a 19-residue N-terminal helical extension (PDB IDs 3ZGO and 5Y5N), similar to the AlphaFold model. The deacetylase SIRT2-type domain (amino acids 53–357) includes amino acids associated with the NAD<sup>+</sup>-binding domain, the Zn<sup>2+</sup>-binding module, and the key catalytic amino acid H187 (Fig. 1B). The highly conserved catalytic core domain adopts an elongated shape containing a classical open  $\alpha/\beta$  Rossmann-fold structure, present in many NAD(H)/NADP(H)-binding enzymes, and a smaller globular domain composed of two insertions in the Rossmann fold (23) (Fig. 1B).

The Rossmann fold consists of six  $\beta$ -strands that form a parallel  $\beta$ -sheet and six  $\alpha$ -helices that pack against the  $\beta$ -sheet. It contains many of the hallmarks of a typical NAD<sup>+</sup>-binding site, including a conserved Gly-X-Gly sequence important for phosphate binding, a pocket to accommodate an NAD<sup>+</sup> molecule, and polar residues responsible for ribose group binding. The first domain consists of four  $\alpha$ -helices that fold to form the helical module. This module has a pocket lined with hydrophobic residues that intersects the large groove. The second domain contains a small, three-stranded antiparallel  $\beta$ -sheet, an  $\alpha$ -helix, and one zinc atom tetrahedrally coordinated by four cysteine residues (Fig. 1A). The role of the zinc ion appears structural, as it is postulated to be required for holding together the  $\beta$  strands. In support of the zinc ion acting as a structural entity, mutation of the four coordinating cysteines to alanine in an SIRT2 yeast homolog completely abrogates deacetylase activity (24).

Between the two domains exists a deep cleft where the enzyme active site is located and where both NAD<sup>+</sup> and N-acetyl-lysine substrates bind (Fig. 1B). The amino acids involved in catalysis and the reactive groups of both bound substrate molecules are buried within a protein tunnel in the cleft (see “Structural insights into catalysis”). This region of the enzyme contains the highest sequence conservation among SIRT2s. Figures 1C and D showcase the main conformations adopted by SIRT2 during its catalytic cycle, commented on in detail in “Structural insights into catalysis”.

##### Quaternary structure

SIRT2 has been isolated by size-exclusion chromatography as a homotrimer from cultured human cell extracts, similarly to its yeast ortholog Hst2 and to SIRT1 (25). A recent report shows that SIRT2 readily dimerizes (as well as, to a minor extent, trimerizes) in solution and in cells and that dimerization affects its activity. The ability of SIRT2 to dimerize appears to be linked to its deacetylase activity, but not to its long-chain fatty acid deacylation (26). Multiple SIRT2 crystal structures present a variety of oligomerization states within

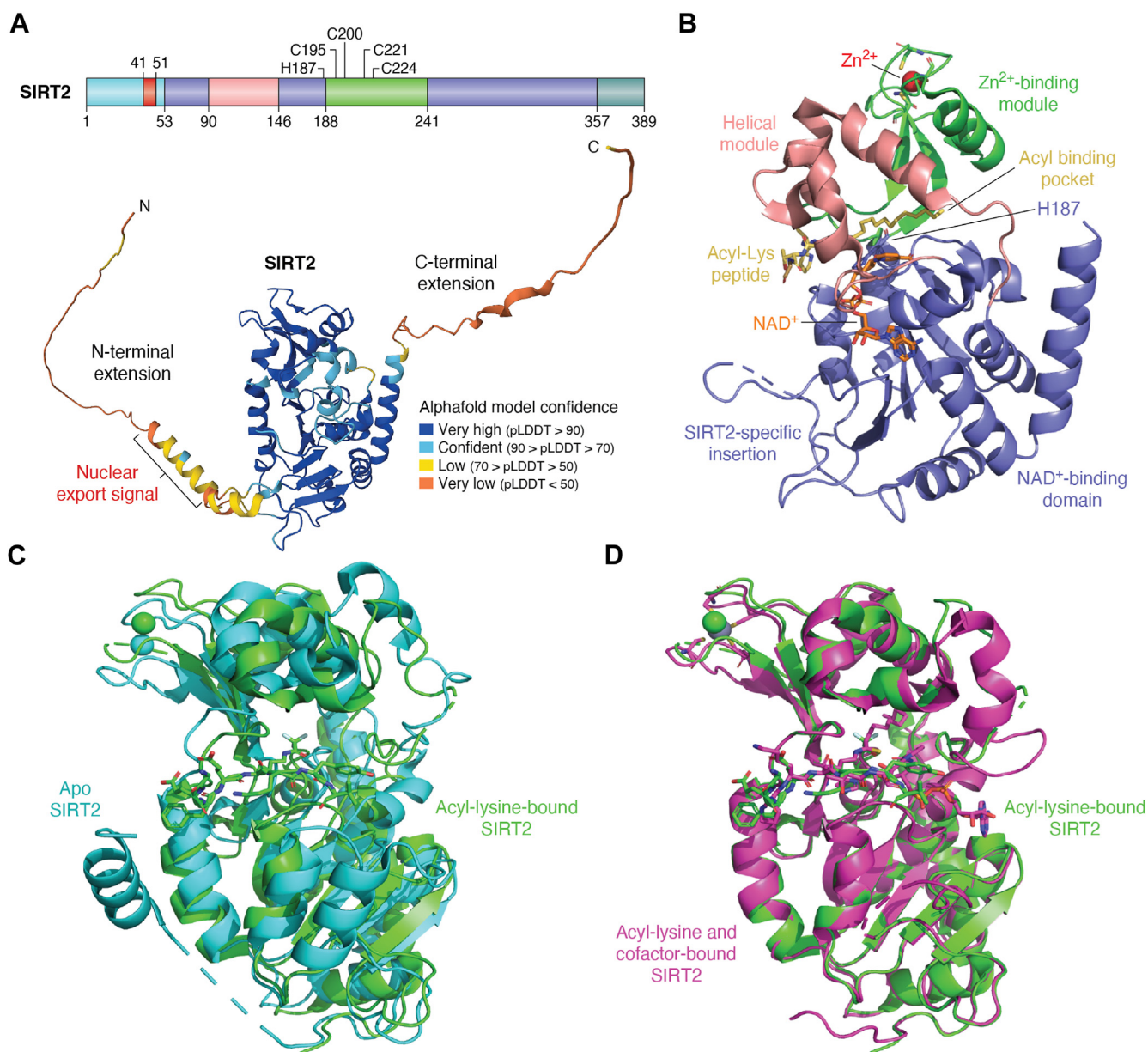


**Figure 1. Overview of SIRT2 structure.** *A*, top: scheme displaying the subdomains in SIRT2, highlighting key residues for catalysis (H187) and stability (C195, C200, C221, and C224). *Bottom*: SIRT2 AlphaFold predicted structure (<https://alphafold.ebi.ac.uk/entry/Q8IXJ6>) in the same orientation as in (*A*), represented in cartoon mode, colored according to the model confidence metric pLDDT (AlphaFold produces a per-residue estimate of its confidence on a scale from 0 – 100; the lower confidence bands may be associated with disorder). The RMSD between SIRT2 AlphaFold predicted structure and PDB ID 4X3P is 0.7 Å. *B*, SIRT2 domain structure organization and main features colored as indicated (PDB ID 4X3P). *C*: comparison of the conformations of apo SIRT2 (PDB ID 3ZGO) and acyl-lysine-bound SIRT2 (PDB ID 5FYQ). *D*: comparison of the conformations of acyl-lysine-bound SIRT2 (PDB ID 4X3P) and acyl-lysine- and cofactor-bound SIRT2 (PDB ID 4X3P). The orientation of SIRT2 in (*C*) and (*D*) is rotated 90 ° clockwise to (*B*). Created with PyMOL(TM) Molecular Graphics System, Version 2.5.0., Schrodinger, LLC and with <https://biorender.com/>. NES, nuclear export signal.

their asymmetric units (see [https://www.rcsb.org/groups/sequence/polymer\\_entity/Q8IXJ6](https://www.rcsb.org/groups/sequence/polymer_entity/Q8IXJ6)). As noted above, most of the structures solved presented truncated termini, which could affect SIRT2 assembly.

To date, the only available full-length SIRT crystal structure corresponds to the yeast Hst2 protein. Interestingly, it revealed a homotrimer in the crystal lattice as well as in solution (27). The analysis of the structure showed that the seven N-terminal residues of Hst2 are binding in the active site cleft of a symmetry-related molecule in the crystal structure. In the

same work, it was shown that the same seven N-terminal residues are required for Hst2 trimer formation in solution, suggesting a role for this region in oligomerization state maintenance. Strikingly, the addition of *N*-acetyl-lysine peptides displaced the binding of the N terminus from the Hst2 active site cleft, disrupting trimer formation. Altogether, these data are compatible with a model in which the N-terminal region of the SIRT may function as an autoinhibitor until the appropriate substrate binds and displaces the N terminus, hence, activating the SIRT.

### Structural insights into catalysis

While the discovery and early characterization of SIRT activity involved knock-out and overexpression models, kinetic studies using recombinant SIRTs and acetylated peptides were later used to establish the catalytic mechanism of deacetylation (28). Despite the early focus on deacetylation, in the last few years, it has been discovered that SIRTs can perform a varied list of deacylations of longer acyl chains—including demalonylation, de-4-oxononanoylation, demyristoylation, and numerous other long-chain fatty acid deacylations. SIRT2 additionally exhibits mono-ADP ribosylation activity (see ref. 17 for a comprehensive list and Fig. 2A). Structural efforts later provided support for the conclusions from kinetic studies and expanded understanding of the catalytic mechanism of SIRT deacetylation (29–32). Figures 1C, 2, B and C and 3, A and B illustrate the different steps of the catalytic mechanism and associated conformational changes.

It has been proposed that the acylated substrate binds first (32). The binding event induces a movement of the  $Zn^{2+}$ -

binding module that opens the *N*-acyl-lysine-binding site (Fig. 1C). Comparison of the apo structure (PDB ID 3ZGO), a representative structure of SIRT2/trifluoroacetyl-lysine peptide (PDB ID 5FYQ) and several longer acyl-lysine/SIRT2 structures (PDB IDs 4Y6L, 4Y6O, 4R8M, 6L65) reveals a hydrophobic cavity that can accommodate the different-sized acyl groups through an induced fit (Figs. 1C and 2C). The acyl group is held in a relatively fixed position during catalysis through a water-mediated acyl interaction (observed in PDB IDs 4Y6L, 4Y6O and 6L65), as can be seen in subsequent steps, while conformational changes happen at the myristoyl-ribose linkage (29–32). Nevertheless, the acyl-binding pocket can accommodate different acyl trajectories, in line with the wide array of acyl substrates that can be deacylated by SIRT2 (Fig. 3, A and B).

The cofactor (NAD<sup>+</sup>) binds the acetyl-lysine–SIRT2 complex prior to any catalytic event (32). Again, the binding triggers a conformational change, this time of the cofactor-binding loop, which was highly flexible and disordered in the previous

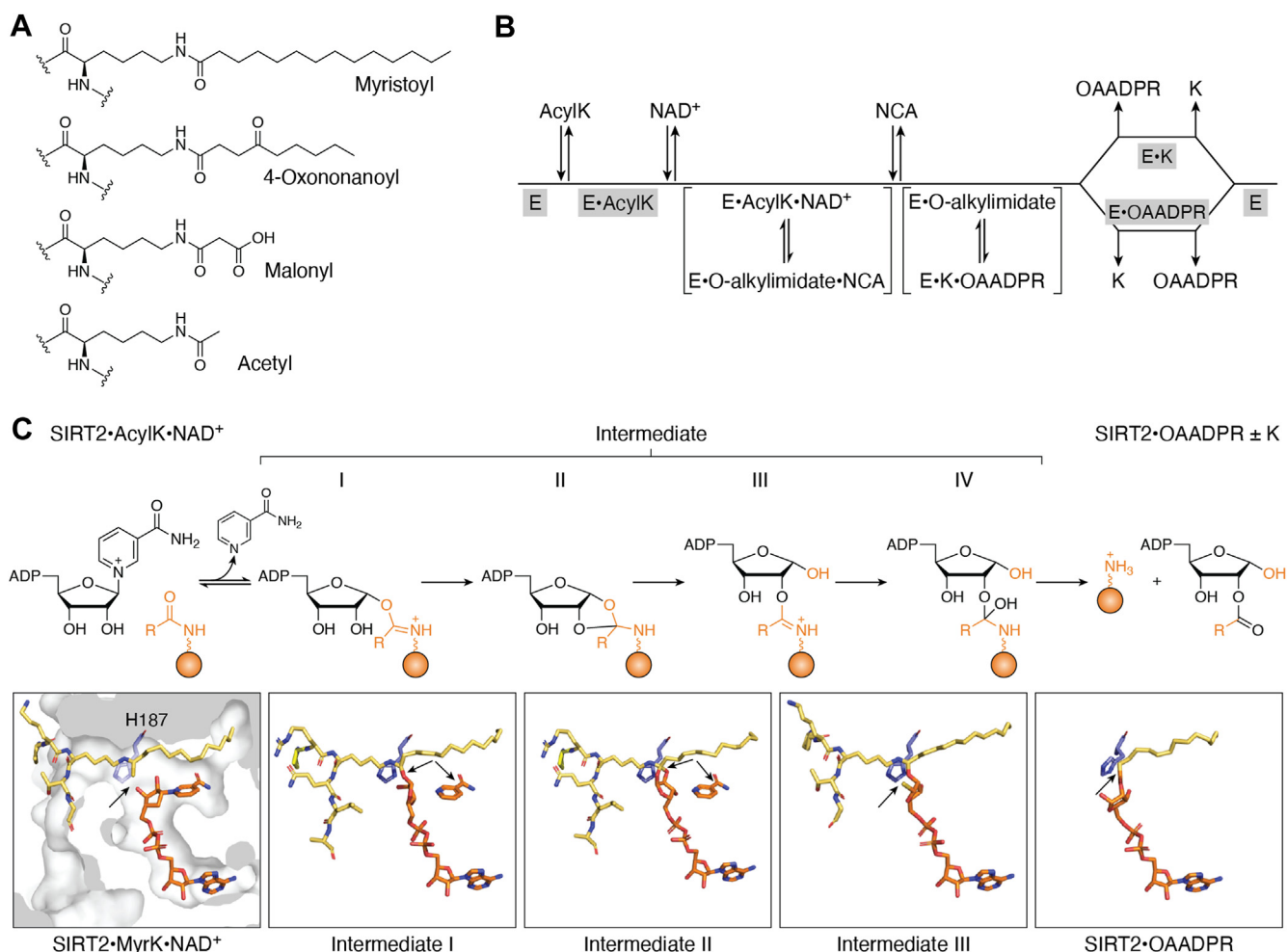


**Figure 2. Overview of SIRT2 structural bases for catalysis.** A, chemical structures of representative acyl-lysine SIRT2 substrates. B, SIRT2 deacylation kinetic scheme. Adapted from reference 31. C, proposed SIRT2 deacylation mechanism (top), with structures representing states and intermediates, as indicated (bottom, arrows indicate the location of the distinct features among structures). Structures used are as follows: SIRT2/acyl-lysine/NAD<sup>+</sup> (PDB ID 4X3P), intermediates I and II (PDB ID 6L71), intermediate III (PDB ID 4X3O), SIRT2/OAADPr (O-Acetyl-ADP-ribose) (PDB ID 4Y6Q). (B and C) have been adapted from reference 31. Created with PyMOL(TM) Molecular Graphics System, Version 2.5.0., Schrodinger, LLC.; ChemDraw 21.0.0; and with <https://biorender.com/>. NCA, nicotinamide.

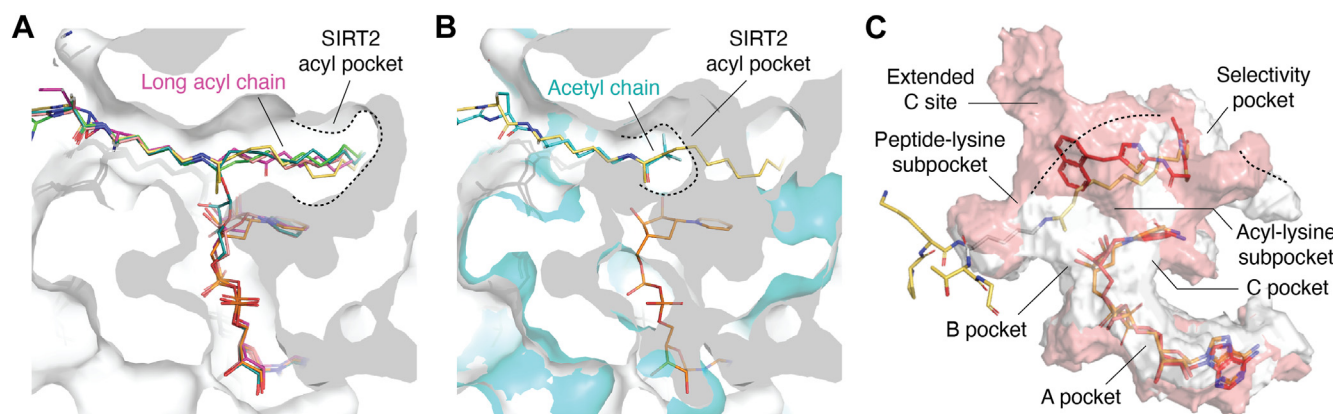


**Figure 3. SIRT2 active site architecture and organization.** A, comparisons of the induced opening (*dashed* line and sliced surface) of the acyl pocket between long acyl chains (PDB ID 4X3P, as in Fig. 2B; PDB ID 4R8M, *green*; PDB ID 5G4C, *magenta*; PDB ID 6L66, *light pink*; PDB ID 6L71, *dark green*) and (B) an acetyl chain (PDB ID 5FYQ, *cyan*), respectively. C, surface representation of the active site of SIRT2/acyl-lysine/NAD<sup>+</sup> (*white* surface/*yellow* sticks/*orange* sticks, respectively, PDB ID 4X3P, see Fig. 1A for comparison) and SIRT2/NAD<sup>+</sup>/SirReal2 (*red* surface/*red* sticks/*red* sticks, respectively, PDB ID 4RMG), designating the individual subsites referred to in the text. Significant protrusions of the SirReal2-bound pocket are shown in *dashed* lines. The surface of the binding pockets was generated using the DoGSiteScorer algorithm at <https://proteins.plus>. Created with PyMOL(TM) Molecular Graphics System, Version 2.5.0., Schrodinger, LLC.; ChemDraw 21.0.0; and with <https://biorender.com/>.

states. The change allows productive binding of the cofactor (PDB IDs 4X3P, 5G4C, 6L66). Overall, the binding of the cosubstrates provokes closure of the cleft around both ligands (Figs. 1C and 2C).

The ternary complex sets the stage for the chemistry (Fig. 2C): the acyl group is transferred to ADP-ribose and then the deacylated substrate and *O*-acyl-ADP-ribose are released. The first step of the reaction is nucleophilic attack of the acyl carbonyl on the C1' of the ribose displacing nicotinamide, which is released and exits the active site through the nicotinamide exit tunnel (opposite the acyl-lysine entrance) (29–32). This forms alkylimidate intermediate (I).

The catalytic residue H187, which acts as a proton acceptor, activates the 2'-OH of the ribose. The 2'-OH then attacks the alkylimidate carbon to form the bicyclic intermediate II. While intermediates I and II had been previously observed in other SIRTs (29), PDB ID 6L71 captures a mixture of both states for SIRT2 (33). PDB ID 6L71 and the related structures (PDB IDs 6L65, 6L66 and 6L72) are part of a time-lapse crystallography approach, which has been utilized to provide relevant insights into the catalysis of different enzymes (34).

The bicyclic intermediate is next attacked by a water molecule yielding the products, the deacylated lysine and *O*-acyl-ADP-ribose. Structural efforts and mass spectrometry have provided evidence of the existence of two additional intermediates in the mechanism (29, 32, 35), including an alkylimidate ion (intermediate III, PDB 4X3O), and predicted the existence of the tetrahedral intermediate IV, formed by the reaction of intermediate III with the aforementioned water molecule. Kinetic experiments support the view that the nucleophilic attack of the 2'-OH on intermediate I is the rate-determining step for SIRT2 long acyl chains, while for short acyl ones, the rate-determining step is the nicotinamide release (29, 32).

For SIRT2, there is a decrease in the reaction rate with increasing acyl substrate chain length. For SIRT2, there is slower turnover with increasing acyl substrate chain length.

SIRT2 catalytic efficiency ( $K_{\text{cat}}/K_m$ ) is less for deacetylation, but the  $K_m$  for acyl-lysine substrate is lower in value (binds tighter) with the increase of the acyl substrate chain length (32). Hence, these structures provide a rationale for the inverse proportionality of  $K_{\text{cat}}$  and  $K_m$  when increasing the acyl chain length. In other words, acetyl-lysine may be more loosely bound and rapidly deacetylated; conversely, a longer, more tightly bound acyl-lysine like myristoyl-lysine is more slowly deacetylated (30, 32, 36). In this sense, longer acyl-lysine substrates are more sensitive to inhibition by nicotinamide, which could be explained by competition from the reverse reaction (formation of NAD<sup>+</sup>) (32).

### Structural insights into modulation

SIRT2 targeting—given its relevant physiological and pathological roles—has been extensively studied, especially within the last decade. Here we will focus on the structure-based drug discovery and design approaches and, particularly, we will comment on the structures that have provided key insights to the field. We will generally refer to the activity of compounds as “modulation,” since different molecules have been shown to activate, inhibit, or selectively inhibit subsets of SIRT2 functions, for example, inhibit deacetylation but not demyristoylation activity (37–39). In most cases, substrate selectivity has not been evaluated. For a more detailed focus on other aspects of SIRT2 activity modulation, we refer the reader to several recent reviews (40–42).

### SIRT2 modulation and selectivity

A great number of chemically diverse SIRT2 modulators have been reported, and there are different criteria with which one can group them. Here, based on the PDB SIRT2/modulator structures (in some cases with one of the cosubstrates or products), we have clustered them into four different groups: 1) mechanism-based modulators, 2) substrate-mimicking modulators, 3) C pocket-binding modulators, and 4)

selectivity pocket-binding modulators. All SIRT2 modulators bind to one or more of the subpockets identified *via* crystallography and depicted graphically in [Figure 3](#).

#### Mechanism-based modulators

Mechanism-based inhibitors, here termed mechanism-based modulators (MBMs), bind to a target protein and through enzymatic catalysis are transformed into stable intermediates that inhibit the enzyme competitively or reactive species that modify the active site covalently ([43](#)). Structures containing MBMs have been extremely useful for understanding the catalytic mechanism of SIRT2s that was summarized in the previous section. For example, the SIRT2 intermediate III complex step has been captured through an MBM: a 1'-SH-2'-O-myristoyl intermediate resulting from the soaking with NAD<sup>+</sup> of a cocrystal of SIRT2 with a thiomyristoyllysine peptide-based inhibitor ([29](#)) (PDB ID 4X3P, [Fig. 2C](#)). The first reported structure corresponding to SIRT2 with an MBM corresponds to the crystal structure of SIRT2 in complex with an  $\epsilon$ -trifluoroacetyl-lysine-containing macrocyclic peptide

modulator, S2iL5 ([44](#)) (PDB ID 4L3O), which has high binding affinity and good SIRT2 deacetylase inhibition activity. This structure displays very similar interactions ([Fig. 4A](#)) to those observed in the SIRT2/acetyl-lysine peptide structure (PDB ID 5FYQ, [Fig. 3A](#)), with a partially open acyl-binding pocket due to the shorter acetyl group (in comparison with myristoyl and other longer acyl groups). In addition, S2iL5 interacts with and stabilizes an SIRT2-specific insertion loop (residues 289–304) in the NAD<sup>+</sup>-binding domain, which is disordered in most of the SIRT2/acetyl-lysine peptide structures ([Fig. 4A](#)). PDB ID 6NR0, ([35](#)) presents another representative SIRT2/MBM structure ([Fig. 4B](#)), based on a thiomyristoyllysine (TM). Similar to the case of S2iL5, the glucose-conjugated TM (glucose-TM) analog was designed for improving the aqueous solubility in respect to the poorly soluble parent compound. The structure is very similar to the previously discovered and crystallized SIRT2 MBM, BHJH-TM1 ([30](#)) (PDB ID 4R8M), displayed in [Figure 3B](#). Of note, the TM scaffold has been used to design proteolysis targeting chimera (PROTAC) SIRT2 degraders ([45](#)), bifunctional molecules with one end of the molecule binding to the target protein (*i.e.*, TM

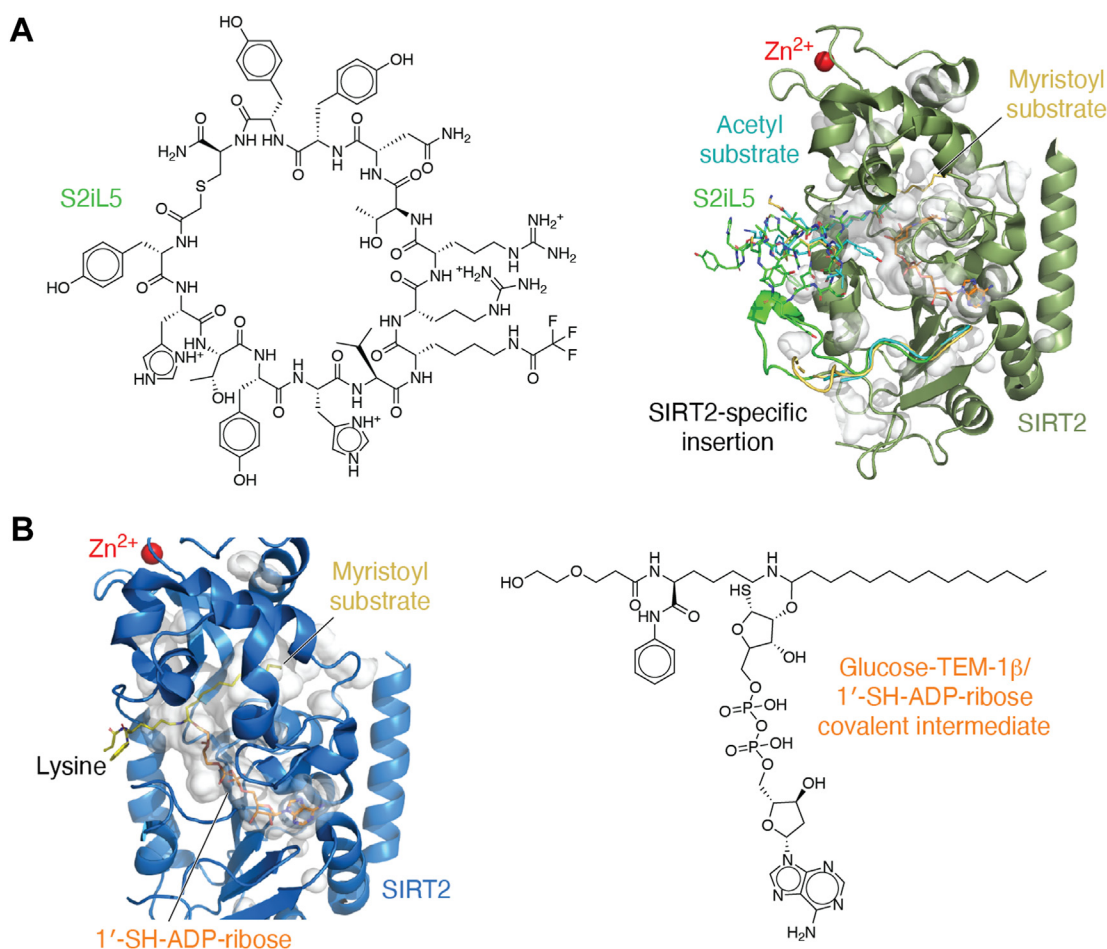


**Figure 4. Structural bases for SIRT2 modulation (I).** A, comparison of the SIRT2/S2iL5 structure (dark green cartoon and white inner surface/green sticks, respectively, PDB ID 4L3O) with representative acyl-K substrates (acetyl-K in cyan, PDB ID 5FYQ; myristoyl lysine in yellow and NAD<sup>+</sup> in orange sticks, PDB ID 4X3P), with Zn<sup>2+</sup> as red sphere in all. B, SIRT2 (blue cartoon and white inner surface) complex with covalent intermediate between mechanism-based inhibitor glucose-TM-1beta (yellow) and 1'-SH ADP-ribose (orange). Created with PyMOL(TM) Molecular Graphics System, Version 2.5.0., Schrodinger, LLC.; ChemDraw 21.0.0; and with <https://biorender.com/>.

enabling SIRT2 binding) and the other end recruiting an E3 ubiquitin ligase, leading to the ubiquitinylation and degradation of SIRT2, with the resulting inhibition of deacetylation.

#### Substrate-mimicking modulators

Substrate-mimicking modulators, here referred to as substrate-mimicking modulators (SMMs), are closely related to MBMs. In this case, the rationale is that the use of chemical groups mimicking the acyl-lysine peptide substrate may yield more “drug-like” scaffolds and prove to be competitive inhibitors to the peptide substrate. Figure 5A illustrates several

SMM chemotypes. The first structural work describing SMMs shows the crystal structure of SIRT2 in complex with a 1,2,4-oxadiazole analog and ADP-ribose (46) (PDB ID 5MAR). Indeed, this scaffold occupies a similar space as the acyl moiety of a substrate (Fig. 4A). Structure-guided structure-activity relationship (SAR) studies of *N*-(3-(phenoxymethyl)phenyl)acetamide derivatives with SIRT2 led to the identification of potent leads mimicking the interactions of myristoyllysine substrates (47). Researchers also synthesized 1,2,4-oxadiazole compounds to explore structure-activity relationships (48). Ascorbyl palmitate was identified as a novel SIRT2 inhibitor, mimicking a substrate and inhibiting both deacetylase and

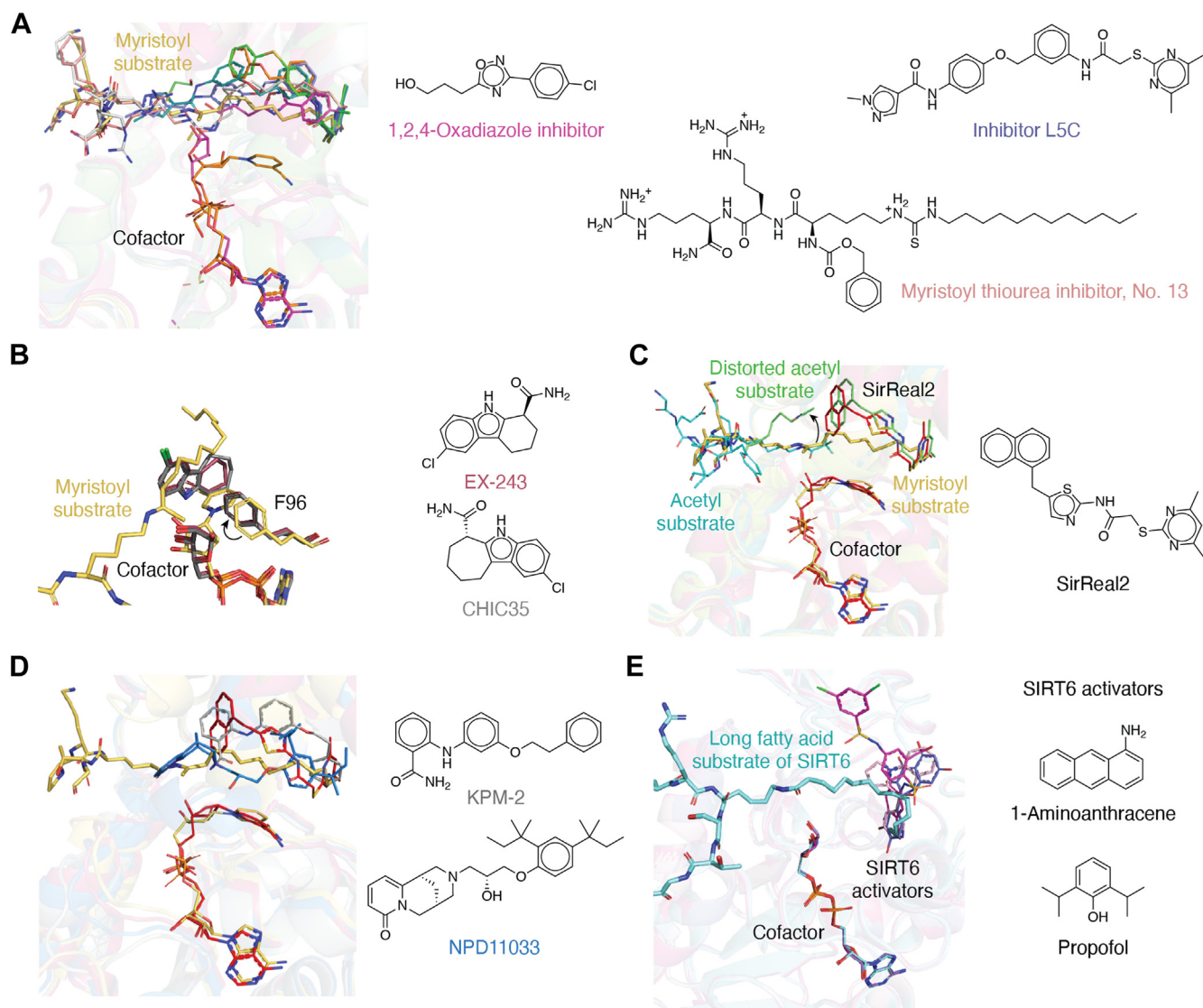


**Figure 5. Structural bases for SIRT2 modulation (II).** A, comparison of several substrate-mimicking inhibitors complexed with SIRT2, with representative inhibitors' chemical structures. Structures: PDB ID 4X3P (as in Fig. 1B), PDB ID 5MAR (magenta), PDB ID 5YQO (violet), PDB ID 5YQL (orange), PDB ID 5YQM (green), PDB ID 5YQN (dark green), PDB ID 7BOS (light pink), PDB ID 7BOT (white). B, comparison of representative C site binders and movement of gatekeeper residue F96 indicated by the arrow. Structures: PDB ID 4X3P (yellow), PDB ID 5D7P (dark red), PDB ID 5D7Q (dark gray). C, comparison of the SIRT2/SirReal2 structures (magenta and green, PDB ID 4RMG and 4RMH, respectively) with representative acyl-lysine substrates (acetyl-lysine in cyan, PDB ID 5FYQ; myristoyl lysine in yellow and NAD<sup>+</sup> in orange sticks, PDB ID 4X3P). D, representative structures of SIRT2 complexes with other selective SIRT2 inhibitors binding in the selectivity pocket (PDB ID 5Y0Z in blue, PDB ID 5Y5N in gray) and compared with the structures in 5C (except PDB ID 4RMH). E, comparison of a SIRT6/myristoyl lysine structure (PDB ID 3ZG6 in cyan) with SIRT6/deacetyl-lysine activator structures (PDB ID 5MF6 in light pink, PDB ID 6QCD in violet, PDB ID 6XV1 in magenta) and the two currently known SIRT2 deacetyl-lysine activator chemical structures. Created with PyMOL(TM) Molecular Graphics System, Version 2.5.0., Schrodinger, LLC.; ChemDraw 21.0.0; and with <https://biorender.com/>.

defatty-acylase activities, contributing to cellular toxicity (49). Finally, Nielsen et al. (50), considering the previous MBMs and structures from intermediate leads (50), have recently developed optimized peptidomimetics with more “drug-like” properties and tight-binding properties. Notably, the lead compounds are capable of inhibiting the demyristoylase activity of SIRT2, which is challenging due to the low  $K_m$  values of myristoyllysine substrates (as detailed in “Structural insights into catalysis”).

#### *C pocket-binding modulators*

As seen in Figure 3, the NAD<sup>+</sup>-binding pocket can be subdivided into three subpockets: A, B and C, binding the adenine ring, the pyrophosphate and two ribose moieties, and nicotinamide, respectively. As noted in “Structural insights into catalysis”, nicotinamide is a natural SIRT modulator, which, when in excess, can promote NAD<sup>+</sup> formation and “re-acetylation” of the peptide lysine. Several nicotinamide-based modulators, such as EX-243 and CHIC35, have been designed (51). After the hydrolysis reaction occurs, F96, the gatekeeper residue, blocks the nicotinamide exit tunnel of SIRT2. C pocket binders, by virtue of occupying part of the NAD<sup>+</sup> pocket, can distort the conformation of the pocket (Fig. 5B). Thus, they are uncompetitive modulators, and all SIRT/nicotinamide complexes contain either the cofactor NAD<sup>+</sup> or the product analog ADP-ribose. Further, two structures featuring C pocket-binding modulators were obtained through optimized crystallization of SIRT2 and SIRT3 *via* microseed matrix seeding (52).

#### *Selectivity pocket (aka extended C, EC, pocket) binding modulators*

Selectivity pocket-binding modulators were discovered by Rumpf et al. through *in vitro* biochemical screening. Through structure determination, it was observed that this type of compound induces opening of the acyl-binding pocket without triggering closure of the Zn<sup>2+</sup>-binding module (53). Accordingly, the authors dubbed this state as “locked open.” Moreover, these modulators protrude slightly from the acyl-binding pocket (Fig. 3C), and, due to the induced rearrangement into SIRT2, these compounds were named “sirtuin rearranging ligands” (SirReals) (53). Thus, this subpocket has been named the “selectivity pocket,” as the rest of human SIRTs are not inhibited by SirReals. The central scaffold of SirReals is the aminothiazole moiety. Other different chemotypes, such as thienopyrimidinones, have been added to the SirReal toolbox. Importantly, SirReals are noncompetitive inhibitors of acetyllysine peptides, inducing a distorted conformation of the substrate (PDB ID 4RMH, Fig. 5C). SAR studies have explored the possibilities of the SirReal scaffolds, showing improved potency (51, 54).

Currently, 16 PDB entries are available with modulators bound in this selectivity pocket (Table 1.). Of those, five structures are dimers featuring a second ligand-bound chain. These 21 chains were analyzed to identify residues that interact directly, or through a single water, with a selectivity/

EC pocket-bound ligand. In total, electrostatic interactions (comprised of pi-pi stacking, hydrogen bonds, and cation-pi interactions) account for 70 total direct interactions and 19 water-mediated hydrogen bonds.

Across these entries, 11 residues are implicated in pi-pi, hydrogen bond, or cation-pi interactions (Tables 1 and 2, Fig. 6). The selectivity region is largely characterized by hydrophobic residues and inhibitors interact with SIRT2 predominantly through an array of pi-pi stacking interactions. Certain residues Y139, F190, and F234 retain a conserved conformation when interacting with a ligand and represent opportune residues for maintaining conserved interactions when designing new ligands. Additionally, 11 residues are involved in water-mediated hydrogen bond interactions (Table 2). These molecular interactions between small molecules and the residues in the peptide-binding channel and the selectivity pocket could provide insights into the various peptide and acyl chain substrate inhibition selectivity and ultimately predict phenotypes.

The flexibility and substrate promiscuity of SIRT2 are noted as important factors in the context of drug design. Specifically, the observed size of the EC pocket in available PDBs is altered dramatically by the presence of acyl-lysine substrate, ligand, and/or NAD<sup>+</sup>. Several interacting residues are observed to shift dramatically to engage in various ligand-receptor interactions. Further, the prevalence of isoleucine, leucine, proline, phenylalanine, and valine residues present a challenge in the context of pocket hydrophobicity and relative weakness of pi-pi stacking interactions compared with more desirable electrostatic interactions.

Interactions within the EC pocket are predominantly pi-pi stacking, totaling 50 out of 89 observed interactions. These interactions are generally weaker than hydrogen bonds or other electrostatic interactions and are localized in the top of the pocket. Phe96 should be considered a mobile phenylalanine residue which adopts conformations across a 6 Å range to engage in pi-pi stacking interactions (4RMI to 5Y0Z). Phe119 has a more conserved conformation, picking up one of two discrete positions that are 3.6 Å apart, with one exception in 5MAR which sits 3 Å away from the closer grouping. As noted in Table 1, there are five total cation-pi interactions and Phe119 maintains three of them. Tyr139 conformations are well conserved spatially and in orientation, with six of seven within 0.5 Å and only the 5MAT conformation displaced by 3.1 Å. Phe190 interactions are well conserved, with the exception of the 5D7Q conformation which is 4.2 Å from the others. Phe234 is highly conserved with seven interactions where all sidechain conformations are conserved to under 0.5 Å.

Higher impact electrostatic interactions, such as hydrogen bonds, are also conserved, but to a lesser extent. In the case of Arg97, four hydrogen bonds and one cation-pi interaction are observed. While none of these interactions present with a great deal of spatial overlap, two of the three arginine side chains are well overlapped, and all four hydrogen bonds share generally conserved vector orientations. Val233 backbone engages in three hydrogen bonds, with both chains of 5MAR and 5YQO within a 1 Å spread. Water bridging interactions, featuring a

**Table 1**  
Ligand–receptor interactions and water bridging interactions by PDB entry

PDB/compound information			Ligand–receptor interactions		Water bridging interactions		
PDB	Compound/Cofactor/Substrates	Compound ID	Residue	Interaction	Residue	Compound region	Water
4RMG (53)	SirReal2/NAD+	3TE 402	Phe131 Phe190 Phe234	Pi-Pi Pi-Pi Pi-Pi	Pro94	Amide (=O)	A
4RMH (53)	SirReal2/Ac-Lys-H3 peptide	3TE 402	Phe119 Phe131 Phe190 Phe234	Pi-Pi Pi-Pi Pi-Pi Pi-Pi	Pro94	Amide (=O)	A
4RMI (53)	SirReal1/Ac-Lysine-OTC peptide	3TK 402	Phe96 Tyr139 Phe190 Phe234	Pi-Pi Pi-Pi Pi-Pi Pi-Pi			
5D7P chain A (52)	ADPR/EX-234 EC Pocket	OCZ 403	Leu138 Gly141	H-bond H-bond	Asp170	Amide (=O)	A
5D7P chain B (52)	ADPR/EX-234 EC Pocket	OCZ 403	Leu138 Gly141	H-bond H-bond			
5D7Q chain A (52)	ADPR/CHIC35 EC Pocket	4I5 404	Leu138 Gly141	H-bond H-bond			
5D7Q chain B (52)	ADPR/CHIC35 EC Pocket	4I5 404	Leu138 Gly141 Phe190	H-bond H-bond Pi-Pi			
5DY4 (51)	SirReal2 brominated Gen 2/NAD+	5GN 402	Phe119 Phe131 Tyr139 Phe190 Phe234	Pi-Pi Pi-Pi Pi-Pi Pi-Pi Pi-Pi	Pro94	Amide (=O)	A
5DY5 (107)	SirReal2 probe fragment	5GR 402	Phe96 Phe96 Arg97 Arg97 Arg97 Phe119 Tyr139 Phe190	Pi-Pi Pi-Pi H-bond H-bond Cation-Pi Pi-Pi Pi-Pi Pi-Pi			
5MAR Chain A (46)	ADPR/1,2,4-Oxadiazole inhibitor	7KE 403	Val233	H-bond			
5MAR Chain B (46)	ADPR/1,2,4-Oxadiazole inhibitor	7KE 403	Phe119 Val233	Pi-Pi H-bond			
5MAT Chain A (54)	Thienopyrimidinone inhibitor	7KJ 402	Phe96 Phe119 Tyr139 Phe190 Phe190	Cation-Pi Cation-Pi Pi-Pi Pi-Pi Pi-Pi	Phe131	Pyrimidone (=O)	A
5Y0Z Chain A (56)	NPD11033 inhibitor	8K9 502	Phe96 Phe119	Pi-Pi Cation-Pi			
5Y0Z Chain B (56)	NPD11033 inhibitor	8K9 502	Phe96 Phe119	Pi-Pi Cation-Pi			
5Y5N (55)	3'-phenethyloxy-2-anilinobenzamide	8NO 1002	Phe119 Phe234	Pi-Pi Pi-Pi	Asp95 Gln167 His187 Phe96 His187 Val233	Amide (NH2) Amide (NH2) Amide (NH2) Amide (=O) Amide (NH2) Amide (NH2)	A A A B C C
5YQL (47)	A2I inhibitor	A2I 1001	Phe190 Phe234	Pi-Pi Pi-Pi	Pro94	Amide (=O)	A
5YQM (47)	A29 inhibitor	A2X 402	Phe96 Phe119 Phe190 Phe234	Pi-Pi Pi-Pi Pi-Pi Pi-Pi	Pro94	Amide (=O)	A

**Table 1**—Continued

PDB/compound information			Ligand–receptor interactions		Water bridging interactions		
PDB	Compound/Cofactor/Substrates	Compound ID	Residue	Interaction	Residue	Compound region	Water
5YQN (47)	L55 inhibitor	L55 402	Arg97	H-bond	Arg97	Amide (=O)	A
			Tyr139	Pi-Pi			
			Phe190	Pi-Pi	Gln167	Amide (=O)	A
			Phe235	Pi-Pi	Glu237	Pyrazole (N)	B
5YQO (47)	L5C inhibitor	L5C 402	Arg97	H-bond	Arg97	Amide (=O)	A
			Phe190	Pi-Pi	His187	Amide (=O)	A
			Val233	H-bond			
			Phe235	Pi-Pi			
7T1D Chain A (39)	small molecule 359	E7K 1007	Phe96	Pi-Pi	Glu116	Imidazole (N)	A
			Tyr139	Pi-Pi			
			Phe119	Pi-Pi			
			Phe190	Pi-Pi			
			Phe190	Pi-Pi			
7T1D Chain B (39)	small molecule 359	E7K 1010	Tyr139	Pi-Pi			
			Phe119	Pi-Pi			
			Phe190	Pi-Pi			
			Phe190	Pi-Pi			

Here, all PDB entries featuring EC pocket ligands are presented with identifiers for their ligands, the SIRT2 residues they interact with, and the type of interaction that occurs between each ligand and receptor. For water bridging interactions, a label for each water has been established for clarity in instances when multiple waters within a PDB entry/chain interact with the ligand. Note that Schrödinger Maestro Pi-Pi stacking face-to-face interaction detection has been adjusted from the default of 4.4 Å to 4.5 Å and includes the 7T1D Phe119 pi-pi interaction as a result.

single water, comprise 19 of the 89 identified interactions. These interactions are distributed around the bottom portion of the EC pocket, and except for those associated with Pro94 are not conserved.

Some MBMs and SMMs also reach the selectivity pocket, as seen for KPM-2 (55) (Fig. 5D) and *N*-(3-(phenoxyethyl)phenyl)acetamide derivatives (47) (Fig. 4C), respectively. Finally, screening of the RIKEN natural products depository identified NPD11033 (56) (Fig. 5D). In this case, the different orientation of the compound in comparison to the original SirReals does not allow for binding of acetyl-lysine substrates, resulting in competitive modulation. An important finding in this work is that while NPD11033 inhibits an acetyl-lysine peptide, it is incapable of inhibiting longer acyl chain deacylation. This appears to correlate with the low  $K_m$  values that SIRT2 displays for long acyl chain substrates. Indeed, Nielsen

et al. have developed an inhibition assay with a myristoyllysine substrate and evaluated SirReal2 demyristoylation inhibitory activity, along with other SIRT2 inhibitors (50). They observed no demyristoylation inhibition by SirReal2 in this assay, which may explain why NPD11033 is also unable to inhibit these types of substrates.

SIRT1 activators have been known since the seminal work of Howitz et al. (57). The most effective of these activators is resveratrol, which activated SIRT1 by > 10-fold. The mechanism of the SIRT1 activators seems to be specific for this protein, with a very long (>200 residues) N-terminal extension featuring a three-helix bundle that comprises the binding domain of the activating molecules, not present in the remaining human SIRTs. The mechanism seems to be allosteric, but is not well understood (for review, see ref. (42)).

**Table 2**  
Electrostatic interactions of EC pocket ligands with SIRT2 by residue and interaction type

Residue	All interactions	Pi-pi interactions	H-bond interactions	Cation-pi interactions	Water bridging interactions
Pro94	0	0	0	0	5
Asp95	0	0	0	0	1
Phe96	8	7	0	1	1
Arg97	5	0	4	1	2
Glu116	0	0	0	0	1
Phe119	11	8	0	3	0
Phe131	3	3	0	0	1
Leu138	4	0	4	0	0
Tyr139	7	7	0	0	0
Gly141	4	0	4	0	0
Gln167	0	0	0	0	2
Asp170	0	0	0	0	1
His187	0	0	0	0	3
Phe190	16	16	0	0	0
Val233	3	0	3	0	1
Phe234	7	7	0	0	0
Phe235	2	2	0	0	0
Glu237	0	0	0	0	1
Total	89	50	15	5	19

PDB entries for SIRT2 featuring EC pocket ligands, totaling 16, were analyzed for all chains, totaling 21. Electrostatic interactions were counted such that multiple interactions with a single residue each count as one. The most conserved sidechain/interaction conformations are visualized in Figure 6.

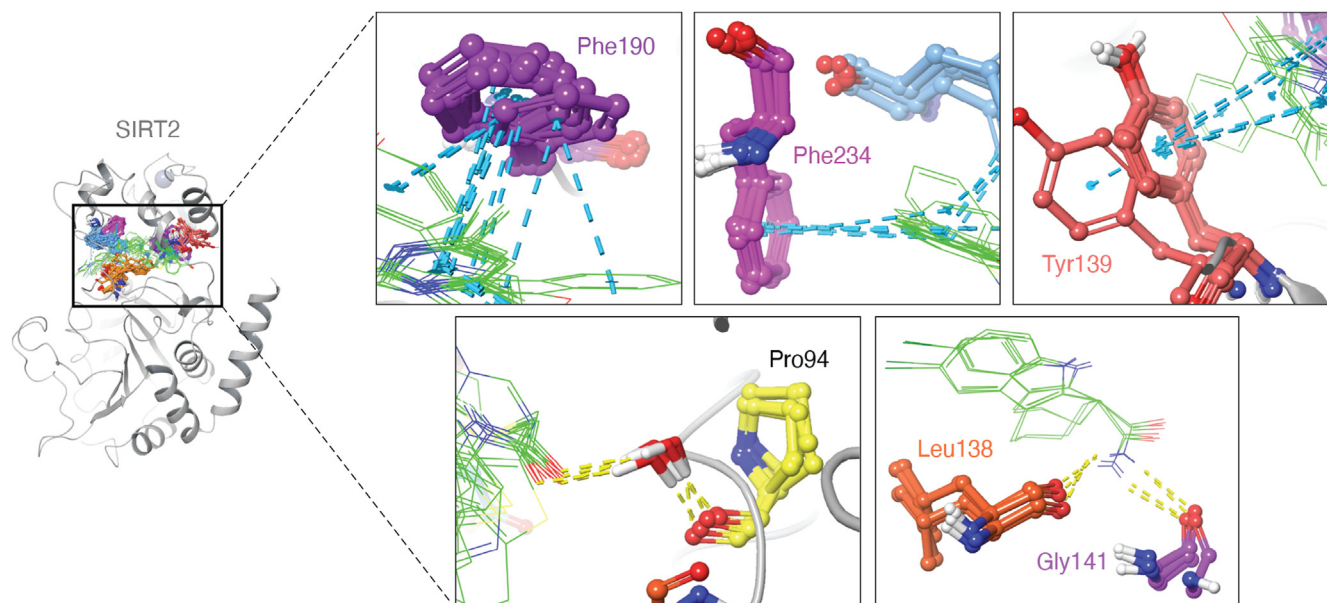


**Figure 6. Visualization of select conserved SIRT2–ligand interactions.** Here, the conserved pi–pi stacking interactions (*blue* dashed lines) between small molecules (*green*; wire frame) and Phe190, Phe234, and Tyr139, the water-mediated hydrogen bond (*yellow* dashed lines) between small molecules and the Pro94 backbone, and direct hydrogen bonds between small molecules and Gly141, Leu138 are highlighted. Certain residues, such as Tyr139 and Phe234 retain a conserved spatial orientation and interaction vectors. Waters that interact with the Pro94 backbone carbonyl also interact with the ligand-based amide carbonyls of 4RMG, 4RMH, 5DY4, 5YQL, and 5YQM. Leu138 and Gly141 backbone interactions are observed for both chains of the 5D7P/5D7Q EC pocket acetamides.

The modulation of the catalytic activity of SIRT2 is substrate-dependent, a feature shared with SIRT6. There seems to be an interdependency between the length of the acyl chain of a substrate and the modulation effect that a small molecule may provide. For instance, SirReals are effective SIRT2 deacetylase inhibitors, but they are not capable of inhibiting demyristoylation. Recent works have found potent SIRT6 activators for deacetylation. Indeed, the MDL derivatives, quercetin and UBCS039, bind SIRT6 in the acyl-binding pocket (58–61) (Fig. 5E). Their binding is compatible with the productive binding of acetyl-containing substrates and activation of SIRT6 (58–61). Given that other noncrystallized SIRT6 activators do work this way (*e.g.*, CL5D (62) and palmitic acid (63)), it is plausible that the MDL derivatives, quercetin and UBCS039, can behave as activators of deacetylase activity and competitive inhibitors of demyristoylation and deacylation of other long acyl substrates.

Recent work by Bi et al. from the Weiser lab describes the two first SIRT2 activators/modulators, 1-aminoanthracene and propofol (64) (Fig. 5E), likely working in a similar fashion as the SIRT6 activators described above. 1-Aminoanthracene inhibits SIRT2 activity on acetyl and myristoyl peptides but activates it on a 4-oxononoyl peptide. Meanwhile, propofol inhibits the same substrates as 1-aminoanthracene but activates the removal of decanoyl peptides. Propofol was reported to bind within the selectivity pocket (65), the same site as SirReal compounds (53). Most interestingly, structural modeling and kinetic analysis with these SIRT2 modulators suggest that the shape of the ligand-binding site dynamically changes during the catalytic cycle. Of the two, 1-aminoanthracene is of interest because it has been utilized as

a probe in biochemical and cellular assays, because it is fluorescent. Further crystallographic studies with these compounds may illuminate the dynamics of the acyl-binding pocket and facilitate the tailoring of SIRT2 modulators to address specific pathological scenarios.

### Structural variation and function

Given the pleiotropic roles of SIRT2, it is not surprising that its regulation at the genetic and “environmental” (subcellular location, interacting partners) levels is complex. This is reflected in a good number of known mutations, post-translational modifications, isoforms and polymorphisms, as well as binding partners (proteins, as well as protein–nucleic acid complexes, *e.g.*, nucleosomes, see “Protein interactions”). The next section will present the current state of this evolving topic, focusing on the effects of these changes in SIRT2 structure and function.

### Mutations

Many SIRT2 mutants, where one or more amino acids have been changed, have been described, and their biological activity has been explored ([https://www.uniprot.org/uniprotkb/Q8IXJ6/entry#disease\\_variants](https://www.uniprot.org/uniprotkb/Q8IXJ6/entry#disease_variants)). However, to our knowledge, systematic approaches are missing, except for a recent study regarding the functional significance of somatic SIRT2 mutations in human tumors (66). The authors utilized an integrated structural, functional, and bioinformatics approach and concluded that most mutations disrupted the catalytic activity, arguing that these mutations are functionally significant. The mutations did not affect SIRT2 cellular location or substrate

binding. Overall, they concluded that somatic SIRT2 mutations in human tumors contribute to genomic instability by impairing its function in DNA damage repair. More studies are necessary to corroborate these findings, but the data provides a compelling example of the central role of SIRT2 in biology and pathology.

Other relevant studies have reported reduced deacetylase activity caused by several mutations located in the SIRT2 catalytic core domain (Fig. 1), including residues S53, S98, S100, Q167, D170, S279, T280, S311, and Y315 (67, 68). Mutations at residues E116, E120, F244, Q265, S271, D294 reduced binding of the macrocyclic peptide inhibitor S2iL5 (44). Mutations N168A (cofactor domain) and H187Y (catalytic domain), which alone or in combination abrogate catalytic activity, were assayed in cellular models to verify whether SIRT2-mediated deacetylation is necessary for regulating tubulin activity. Indeed, N168A and H187Y mutants resulted in the inhibition of chromosome condensation and provoked hyperploid cell formation in response to mitotic stress (68, 69). Not surprisingly, mutation at the active site residue H187 has many reported consequences, including inhibition of deacetylase activity toward multiple substrates (69–73).

Other relevant mutations include S364A and S368A, which abolish cyclin/cyclin-dependent kinase (CDK)2-dependent phosphorylation and inhibit the SIRT2-mediated cellular proliferation delay in early metaphase to prevent chromosomal instability; and an S372A mutation reduces SIRT2 phosphorylation and its catalytic activity (67, 71, 74), pointing to a poorly understood regulatory role of the C-terminal region.

### Posttranslational modifications

There are several phosphorylation sites identified in SIRT2, the most studied being S25 in the N-terminal region, S331 within the catalytic core, and S368 and S372 in the C-terminal extension (Fig. 1A). Dephosphorylation of S25 triggers localization of SIRT2 from the cytosol to the nucleus and is necessary for SIRT2 chromatin association upon infection with the bacterium *L. monocytogenes* (75). S25 dephosphorylation is necessary for histone H3K18 deacetylation and transcriptional regulation during infection. Moreover, the authors also identified other phosphorylation sites and PTMs, including 12 serine and two threonine phosphorylation sites, three ubiquitinylation sites, and six acetylation sites. S331 is targeted by the cyclin-dependent kinases, Cdk2 and 5, and its phosphorylation inhibits SIRT2 enzymatic activity (74). S368 is part of a CDK consensus motif that is a substrate of cyclin B/Cdk1, cyclin E/Cdk2, cyclin A/Cdk2, cyclin D3/Cdk4, and p35/Cdk5 (71, 74). S368 is phosphorylated when cells enter S phase, which suggests that this PTM is not acting as a signal for nuclear accumulation of SIRT2, which happens in late G2 (74). SIRT2 phosphorylation at S368 and S372 is known to reduce its ability to deacetylate histones and  $\alpha$ -tubulin (74), interfering with neurite outgrowth in primary neurons. To date, the kinase responsible for the phosphorylation of S372 remains unidentified (71, 74). Research has focused on PTMs of Sirt2, specifically the phosphorylation of S23 and S25 on its N-

terminal tail. Dual phosphorylation at these sites enhances Sirt2's activity towards peptide and protein substrates. The authors propose that this phosphorylation relieves autoinhibition by Sirt2's C-terminal region (76). Peroxynitrite inhibits the deacetylase activity of SIRT1, SIRT2, SIRT3, SIRT5, and SIRT6, correlating with increased tyrosine nitration. While SIRT1 shows peroxynitrite-mediated cysteine sulfenylation, SIRT2, SIRT3, SIRT5, and SIRT6 do not, although SIRT6 likely forms an intermolecular disulfide bond following transient sulfenylation. Therefore, peroxynitrite can posttranslationally modify and inhibit SIRTs (77). Studies explored how diverse cysteine oxidants influence the function of sirtuin enzymes. They found that primarily nuclear SIRTs were modified and inhibited by cysteine S-nitrosation in response to exposure to both free nitric oxide and nitrosothiols. Surprisingly, mitochondrial SIRTs were resistant to inhibition by cysteine oxidants. These results suggest that nitric oxide-derived oxidants may link nuclear and cytosolic SIRT inhibition to aging-related inflammatory disease development (78, 79).

SIRT2 is acetylated by the KAT p300 (80, 81). This acetylation is not mapped, although it is predicted to occur on the C-terminal extension, and it was shown to interfere with the catalytic activity of SIRT2 (80, 81). Hence, the fact that the N- and C-terminal extensions host functional PTMs is in line with the concept that these regions play a role in regulating activity. Capturing the termini regions in an ordered state (e.g., bound to a probe, as seen for SIRT1) (42) could help in designing tools to modulate SIRT2 activity. Finally, SIRT2 can also be modified by cysteine oxidative PTMs but it is unclear which role these PTM have (78).

### Isoforms and polymorphisms

Protein isoforms are highly related gene products that may perform essentially the same biological function, normally generated by alternative splicing or duplication (reviewed in ref. (82)). Isoenzymes are isoforms of an enzyme that may have been generated during evolution in ancestor organisms; hence, they can differ in their biological activity, regulatory properties, temporal and spatial expression, intracellular location, or any combination of the previous. Consequently, the seven human SIRTs can be considered isoenzymes, and there are five reported spliced RNAs with potential to encode human SIRT2 isoforms in the Genbank sequence database. However, only three have been shown to express proteins (83). The longer, predominantly cytoplasmic SIRT2 isoform 1 (SIRT2.1) consists of 389 amino acids, including an NES (20) and catalytic deacetylase domain (see Fig. 1A). The shorter cytoplasmic isoform 2 (SIRT2.2) lacks the first 37 N-terminal amino acids but includes all amino acids associated with the NES and the deacetylase domain. No catalytic differences have been reported between SIRT2.1 and SIRT2.2. One report points towards C terminus as an autoinhibitory region, and elimination of this segment enhances deacetylase activity. Additionally, truncation of the N terminus accelerates nucleosome deacetylase activity but reduces peptide substrate deacetylation (76). Isoform 5 (SIRT2.5) is 319 amino acids; its N-terminal residues

6 to 76 are replaced by an arginine. As a result, it lacks the NES motif present in the cytoplasmic isoforms and is predominantly found in the nucleus (83–85). SIRT2.5 is catalytically inactive in cell-free assay (83), but it is not yet clear whether this is an intrinsic property of the isoform or a confounding property of the recombinant protein used in the assays.

All residues known to be essential for catalysis are present in isoform 5. The only structurally relevant element missing is  $\alpha$ -helix  $\alpha$ 1 of the NAD<sup>+</sup>-binding Rossmann fold. While structural modeling suggests the overall structure should not be strongly affected, its more exposed N-terminal region of the catalytic core (starting at residue 76, Fig. 1A) may suggest lower structural stability in comparison to isoforms 1 and 2 (83). CobB, a bacterial sirtuin homolog, lacking the equivalent  $\alpha$ -helix in the Rossmann fold, is catalytically active (86). Purified SIRT2.5 binds to the SIRT2 partner p300, and its binding is enhanced by NAD<sup>+</sup>, so it might mediate nuclear protein interactions, possibly in a cofactor-dependent manner (83). Recent studies have shown that it may have regulatory roles: interleukin-4 treatment triggers overexpression of isoform 5 in human macrophage cells and results in an allergic and asthmatic phenotype (85). Moreover, isoform 5 inhibits hepatitis B virus replication, possibly through epigenetic modification of the viral covalently closed circular DNA *via* direct and/or indirect association with histone lysine methyltransferases (84).

As noted in “Mutations”, there is relatively little information on SIRT2 single nucleotide polymorphisms (SNPs). A recent study examined the occurrence of SNPs in cancer patients (66), and R42P, P128L, P140H, R153C, A186V, and F190V were found to be highly conserved and deleterious to SIRT2 deacetylation activity if mutated. Interestingly, all SNPs except the R42P, which is within the NES motif, are located in the catalytic core. An independent study also identified an SIRT2 SNP in the 3'-UTR associated with susceptibility to colorectal cancer (87), although the mechanistic basis for this has yet to be studied. Similarly, SNPs within the SIRT2 locus have been associated with human longevity, myocardial infarction, diabetes, or neurological diseases although the mutations were not within the protein coding sequence (88–91).

### Protein interactions

The most systematic SIRT2 interactome study has been reported by Budayeva and Cristea (92). They utilized a multipronged approach including determining the intracellular localization, identity, and relative stability of SIRT2 interactions. These interactions were transient across the board as could be expected for enzyme-substrate contacts. In addition to the expected interaction with  $\alpha$ -tubulin and other cytoskeleton proteins, it was observed that SIRT2 interacts with proteins involved in membrane trafficking, secretion, and transcriptional regulation.

A recent review has compiled SIRT2-binding partners in the context of gene expression regulation and metabolism (93). Regarding transcription regulation, the interaction of SIRT2 and the homeobox transcription factor HOXA10 in human endometrial cells seems to be enhanced by the bridging effect

of the four half-domains of LIM domain 1 (FHL1) and plays a role in infertility (94). SIRT2 is involved in glucose metabolism, promoting gluconeogenesis through deacetylation of the transcription factor, FOXO1, and the kinase, PEPCK. In addition, SIRT2 can promote glycolysis by interacting with glycolytic enzymes, such as protein kinase B (Akt or PKB), that regulates glucose metabolism through the insulin–PI3K–AKT metabolism pathway (main downstream signaling pathway of insulin action) (95). Other relevant SIRT2-binding partners associated with glycolysis are hexokinase 1, phosphofructokinase, aldolase A, glyceraldehyde-3-phosphate dehydrogenase, phosphoglycerate kinase 1, enolase 1, pyruvate kinase M, and lactate dehydrogenase (96, 97).

Is SIRT2 catalysis driven mainly by the substrate protein's peptide domain that interacts with the SIRT2 active site or does the extended structure of the substrate influence recognition and potentially the deacylation reaction? To probe this issue, Knyphausen et al. produced several natively folded SIRT1, 2, and 3 substrate proteins, containing site-specific lysine acetylations (98). Some acetylated proteins were robustly deacetylated, but others were not. Their data supports the view that substrate recognition by SIRTs is not only affected by the primary sequence surrounding the acetylated lysine, but also to a large extent by the secondary and tertiary structure of the protein substrate.

Beyond substrate interactions, SIRT2 interacting partners can modulate its activity. For instance, a SIRT2–HDAC6 interaction has been reported to be required for SIRT2 activity on tubulin (67).

Along these lines, two recent studies report cryo-EM structures of SIRT6 interacting with the nucleosome (99, 100). The structures reveal multiple interactions of distinct SIRT6 domains with the nucleosome. This can explain why the enzyme is efficient at deacetylating multiple histone H3 acetylation sites in the context of nucleosomes, but not with free acetylated histone H3 protein substrates. While such structures are not yet solved for SIRT2, deacetylation assays also show that SIRT2 is more active against nucleosomal substrates over their peptide counterparts (101). Additionally, the presence of VRK1, an established binding partner of Sirt2 and nucleosomes, can stimulate the nucleosome deacetylation activity of full-length Sirt2 but peptide substrate deacetylations were unaffected by VRK1 (76).

### Discussion and conclusion

This manuscript reviews available crystal structures of SIRT2, demonstrating its ability to bind diverse substrates and informing the design of mechanism- and substrate-based inhibitors targeting multiple domains, including its unique selectivity pocket. However, despite the determination of many crystal structures, numerous open questions remain, especially relating to the development of small molecule modulators, achieving full or partial activation or inhibition of SIRT2, and ultimately translating these effects to different therapeutic applications. Developing drugs that bind to, and modulate, SIRT2 is challenging because of its dynamic structure and

various substrates. Moreover, its ability to deacylate multiple lysine acyl modifications makes SIRT2 complex to model. Better understanding of the acyl groups, the substrate protein sequence, and structural aspects will aid in the design of new small molecule SIRT2 modulators with specific attributes. Despite these challenges, the delineation of different SIRT2 inhibitory mechanisms may provide some hints for developing better small molecule modulators. Of note, the selectivity pocket binders (reviewed in “Selectivity pocket-binding modulators”) slightly protrude outside of the acyl-binding pocket, but the mechanistic basis of their selectivity remains unclear. The role of the disordered termini and the potential for higher order quaternary states (monomer, dimer, and trimer) remain open questions. Deeper insight into these issues may facilitate the development of SIRT2 selective modulators which can be tailored to different pathological scenarios, such as viral infections and cancers, in which either activation or inhibition of SIRT2 may be of therapeutic benefit. Several factors offer opportunities for the development of improved SIRT2 probes and modulators including 1) SIRT2’s inherent flexibility adapting to various substrates and inhibitors and 2) its ability to remove different acyl modifications from lysine residues. This suggests potential for developing inhibitors with varying specificities. 3) the selectivity of small molecules to inhibit different acyl chains on peptide substrates. This highlights the possibility of designing inhibitors that target specific SIRT2 acyl activities. 4) the discovery of different SIRT2 inhibitory mechanisms. This provides multiple avenues for developing new and improved inhibitors. 5) the potential for higher order quaternary states (e.g., dimers and trimers). This offers the possibility of targeting protein–protein interactions to modulate SIRT2 activity.

The growing number of specific acylated lysine residues revealed in numerous proteins involved in many different cellular processes argues that both acylation and deacylation are critically important regulatory mechanisms (1–3). Within the larger group of KDACs, SIRT deacylase activity targets a very large number of proteins (1–3), impacting many disease states such as bacterial and viral infections, as well as many cancers (14, 39, 102, 103). Therefore, understanding how to modulate SIRT2 with different small molecules could provide novel host targeting mechanisms for treating these diseases and allow for synergistic combinations with other drugs.

The X-ray structures reviewed here provide a glimpse into the various states of SIRT2, illustrating the conformational plasticity that enables this enzyme to recognize a variety of substrates. In addition to structural studies, enzymatic studies have provided insight and mechanistic understanding of SIRT catalysis and modulation, as well as the basis for selectivity among the different isoenzymes. This intrinsic flexibility of SIRT2 poses a challenge in terms of small molecule targeting. Moreover, its ability to deacylate multiple lysine acyl modifications makes SIRT2 difficult to model, making the design of new small molecule SIRT2 modulators with specific attributes challenging.

Despite these challenges, the discovery of different SIRT2 inhibitory mechanisms may provide some hints for developing

improved small molecule modulators. While the selectivity pocket binders extend somewhat beyond the acyl-binding pocket (as discussed in “Selectivity pocket-binding modulators”), the mechanism behind their selectivity is still not fully understood. The amino acids that form the selectivity pocket are very similar among SIRT1-3 (53), making sequence differences among the proteins unlikely as to the basis for the selectivity of SirReals and other compounds toward SIRT2. Structural work over the past decades shows that SIRT isoenzymes differ in acyl channel architecture and dynamics (104), and these differences may contribute to the selectivity of binders.

There appears to be a relationship between the length of the acyl chain of a substrate and the modulatory effect that a small molecule may provide on deacylase activity. For instance, SirReals are effective SIRT2 deacetylase inhibitors, but they do not inhibit demyristoylation. Thus, the SIRT2-binding affinity of a myristoylated substrate might be stronger than that of SirReals (suggested by the larger number of hydrophobic contacts of a myristoylated substrate to the binding site in SIRT2). Figure 3 and 5 show clearly that SirReal2 and a myristoylated substrate open the acyl-binding pocket similarly.

We would argue that the merging of the SirReal core with SMM moieties extending into the peptide-lysine subpocket (e.g., inhibitor L5C, Fig. 5A) could allow such compounds to inhibit competitively longer acyl chain deacylation by improving compound affinity. This may be the case for the thiourea-based  $\epsilon$ -N-acyl-lysine mimic compound 13 (Fig. 5B) that outcompetes myristoyl substrates (50). Along these lines, such inhibitors may also have the added benefit that in matching the “substrate envelope,” they may be less prone to or be more resilient to resistance mutations arising in cancer, as mutations reducing a substrate binding might reduce enzyme activity. This concept, initially developed for the case of HIV-1 protease, has also been tested for cancer proteins (105).

Activation of SIRT2 deacetylation with small molecules, as suggested by the SIRT6 structural data (Fig. 5E), could be related to the degree to which the remaining part of the inducible acyl-binding pocket is occupied. Indeed, these molecules inhibit demyristoylation. Given the high resolution of SIRT2 crystals (38 out of 39 structures diffracting at 2.52 Å or better), it can be envisioned that crystallographic fragment screening, either with an acetyl substrate or a SirReal-type small molecule, could guide the development of moieties for optimal filling of the acyl-binding pocket and modulation of SIRT2 activity. This technique is known to be useful for finding hot and warm binding spots in proteins (106).

In a recent SIRT6/nucleosome structure (PDB ID 8F86), the N-terminal region is observed wrapping around the outer surface of SIRT6, while the active site is occupied by the histone H3-lysine-thio-ADP ribose covalent adduct (100). Hence, this SIRT6 structure might present an “activated” SIRT, indirectly supporting the previous hypothesis about the auto-inhibitory role of the trimeric assembly. Given the molecular weight of such a trimer complex (~120 kDa), cryo-EM could

be amenable to solve such a structure for full-length SIRT2, with the benefit of the sample being in solution and with the capability to resolve the heterogeneity induced by the flexible termini. A SIRT2 trimer structure, if confirmed that it represents an inactive form of the enzyme, could represent an appealing target for SIRT2 inhibition. Small molecules that stabilize the “inactive” trimer could provide an alternative mechanism for the modulation of SIRT2 activity.

It is important to consider other factors that can regulate enzymatic activity *in vivo*. For instance, despite having relatively similar hydrophobic pockets, SIRT2 and SIRT3 display varying catalytic efficiencies with the same acylated substrate types (32), which suggest the existence of additional factors not explained by the previous structural-kinetic relationships. While the dynamics of binding of the cosubstrates could be a factor (*e.g.*, the highly flexible cofactor-binding loop), other factors outside of the structural-kinetic relationships may influence activity, including 1) allosteric effects from the full-length substrates with regulatory termini (*e.g.*, monomer to trimer equilibrium, discussed above), 2) effect of PTMs on activity, 3) the effect and role of binding to other proteins, and 4) subcellular compartmentalization. The literature presents a detailed picture of the evolutionary path driving SIRT2s. Each SIRT has evolved to operate in a subcellular compartment where changes in NAD<sup>+</sup> levels will directly affect its activity and substrate preference. For SIRT2, for instance, the low  $K_m$  values for NAD<sup>+</sup> with long chain acyl substrates and the low  $K_m$  values for long chain acyl substrates themselves suggest a housekeeping function to limit the adverse effects of spurious long chain protein acylation from acyl-CoAs. The estimated cytosolic levels of NAD<sup>+</sup> are 10 to 100  $\mu$ M and support this notion (32). Conversely, mitochondrial SIRT3 has a higher  $K_m$  for NAD<sup>+</sup> with all substrates, in concordance with the abundant pool of mitochondrial NAD<sup>+</sup> (~300  $\mu$ M) (32).

In conclusion, the many structures of SIRT2 with diverse binding partners solved in the past decade have increased the understanding of its catalysis, modulation, and selectivity, which provides avenues for the discovery and design of improved probes and modulators (39). An improved toolbox of probes and modulators of SIRT2 activity will help in the understanding of the unknown or partially understood aspects of SIRT2 function (*e.g.*, role of the termini, role of interactions with substrates and other binding partners, or functional consequences of its PTMs).

**Acknowledgments**—We would also like to acknowledge Nicholas Meanwell and Jessica Freeze for reviews and edits on the manuscript. This work was partially supported by NIAID (R44AI114079), and DTRA (MCDC2001-009). Opinions, interpretations, conclusions, recommendations are those of the authors and not necessarily endorsed by the National Institute of Health or Department of Defense.

**Author contributions**—S. P. B., F. X. R., S. R., M. J. T., T. S., J. L. K., and L. W. C. writing—review and editing; S. P. B. and F. X. R. writing—original draft; S. P. B. and F. X. R. visualization; S. P. B., F.

X. R., J. L. K., and L. W. C. methodology; S. P. B., F. X. R., and J. L. K. formal analysis; S. P. B. and F. X. R. data curation; S. R., J. L. K., and L. W. C. project administration; J. L. K. and L. W. C. supervision; J. L. K. and L. W. C. conceptualization; L. W. C. funding acquisition.

**Conflicts of interest**—The authors are employees of Evrys Bio and Conifer Point Pharmaceuticals. Evrys Bio licensed SIRT2 inhibitors from Princeton University in 2014 and has been engaged in optimizing these small molecules for clinical trials, anticipated to commence in late 2025 or early 2026. This review reflects observations and analyses derived from over a decade of public literature study on SIRT2, conducted within the context of Evrys Bio’s drug development efforts. Evrys Bio’s research has been primarily supported by grants and contracts from the National Institutes of Health (NIH) and the Department of Defense (DoD), which are matters of public record. The authors’ employment with Evrys Bio and Conifer Point represents a potential conflict of interest due to their direct involvement in the development of SIRT2 inhibitors. However, the authors have strived to provide an objective and comprehensive review of the structural biology of SIRT2, based on published research and independent analysis. This potential conflict of interest, arising from employment and drug development activities, is disclosed to ensure transparency and allow readers to assess the information presented with full awareness of these affiliations.

**Abbreviations**—The abbreviations used are: KDAC, lysine deacetylase; MBM, mechanism-based modulator; NES, nuclear export signal; PDB, protein data bank; SAR, structure-activity relationship; Sir2, silent information regulator 2; SIRT2, sirtuin 2; SMM, substrate-mimicking modulator; SNP, single nucleotide polymorphism.

## References

- Komaniecki, G., and Lin, H. (2021) Lysine fatty acylation: regulatory enzymes, research tools, and biological function. *Front. Cell Dev. Biol.* **9**, 717503
- O’Garro, C., Igbineweka, L., Ali, Z., Mezei, M., and Mujtaba, S. (2021) The biological significance of targeting acetylation-mediated gene regulation for designing new mechanistic tools and potential therapeutics. *Biomolecules* **11**, 455
- Ali, I., Conrad, R. J., Verdin, E., and Ott, M. (2018) Lysine acetylation goes global: from epigenetics to metabolism and therapeutics. *Chem. Rev.* **118**, 1216–1252
- Dokmanovic, M., Clarke, C., and Marks, P. A. (2007) Histone deacetylase inhibitors: overview and perspectives. *Mol. Cancer Res.* **5**, 981–989
- Rine, J., and Herskowitz, I. (1987) Four genes responsible for a position effect on expression from HML and HMR in *Saccharomyces cerevisiae*. *Genetics* **116**, 9–22
- Kennedy, B. K., Austriaco, N. R., Zhang, J., and Guarente, L. (1995) Mutation in the silencing gene SIR4 can delay aging in *S. cerevisiae*. *Cell* **80**, 485–496
- Gold, D. A., and Sinclair, D. A. (2022) Sirtuin evolution at the dawn of animal life. *Mol. Biol. Evol.* **39**, msac192
- Opazo, J. C., Vandewege, M. W., Hoffmann, F. G., Zavala, K., Melendez, C., Luchsinger, C., *et al.* (2023) How many sirtuin genes are out there? Evolution of sirtuin genes in vertebrates with a description of a new family member. *Mol. Biol. Evol.* **40**, msad014
- Frye, R. A. (2000) Phylogenetic classification of prokaryotic and eukaryotic Sir2-like proteins. *Biochem. Biophys. Res. Commun.* **273**, 793–798
- Flick, F., and Lüscher, B. (2012) Regulation of sirtuin function by posttranslational modifications. *Front. Pharmacol.* **3**, 29
- Brachmann, C. B., Sherman, J. M., Devine, S. E., Cameron, E. E., Pillus, L., and Boeke, J. D. (1995) The SIR2 gene family, conserved from

- bacteria to humans, functions in silencing, cell cycle progression, and chromosome stability. *Genes Dev.* **9**, 2888–2902
12. Houtkooper, R. H., Pirinen, E., and Auwerx, J. (2012) Sirtuins as regulators of metabolism and healthspan. *Nat. Rev. Mol. Cell Biol.* **13**, 225–238
  13. Alqarni, M. H., Foudah, A. I., Muharram, M. M., and Labrou, N. E. (2021) The pleiotropic function of human sirtuins as modulators of metabolic pathways and viral infections. *Cells* **10**, 460
  14. Chalkiadaki, A., and Guarente, L. (2015) The multifaceted functions of sirtuins in cancer. *Nat. Rev. Cancer* **15**, 608–624
  15. Hong, J. Y., and Lin, H. (2021) Sirtuin modulators in cellular and animal models of human diseases. *Front. Pharmacol.* **12**, 735044
  16. Inoue, T., Hiratsuka, M., Osaki, M., and Oshimura, M. (2007) The molecular biology of mammalian SIRT proteins: SIRT2 in cell cycle regulation. *Cell Cycle* **6**, 1011–1018
  17. Wang, M., and Lin, H. (2021) Understanding the function of mammalian sirtuins and protein lysine acylation. *Annu. Rev. Biochem.* **90**, 245–285
  18. Zhang, H., Dammer, E. B., Duong, D. M., Danelia, D., Seyfried, N. T., and Yu, D. S. (2022) Quantitative proteomic analysis of the lysine acetylation reveals diverse SIRT2 substrates. *Sci. Rep.* **12**, 3822
  19. Terwilliger, T. C., Liebschner, D., Croll, T. I., Williams, C. J., McCoy, A. J., Poon, B. K., et al. (2023) AlphaFold predictions are valuable hypotheses and accelerate but do not replace experimental structure determination. *Nat. Methods* **21**, 110–116
  20. North, B. J., and Verdin, E. (2007) Interphase nucleo-cytoplasmic shuttling and localization of SIRT2 during mitosis. *PLoS One* **2**, e784
  21. Eldridge, M. J. G., Pereira, J. M., Impens, F., and Hamon, M. A. (2020) Active nuclear import of the deacetylase Sirtuin-2 is controlled by its C-terminus and importins. *Sci. Rep.* **10**, 2034
  22. Sanders, B. D., Jackson, B., and Marmorstein, R. (2010) Structural basis for sirtuin function: what we know and what we don't. *Biochim. Biophys. Acta* **1804**, 1604–1616
  23. Finnin, M. S., Donigian, J. R., and Pavletich, N. P. (2001) Structure of the histone deacetylase SIRT2. *Nat. Struct. Biol.* **8**, 621–625
  24. Min, J., Landry, J., Sternglanz, R., and Xu, R. M. (2001) Crystal structure of a SIR2 homolog-NAD complex. *Cell* **105**, 269–279
  25. Vaquero, A., Scher, M. B., Lee, D. H., Sutton, A., Cheng, H. L., Alt, F. W., et al. (2006) SirT2 is a histone deacetylase with preference for histone H4 Lys 16 during mitosis. *Genes Dev.* **20**, 1256–1261
  26. Yang, J., Nicely, N. L., and Weiser, B. P. (2023) Effects of dimerization on the deacetylase activities of human SIRT2. *Biochemistry* **62**, 3383–3395
  27. Zhao, K., Chai, X., Clements, A., and Marmorstein, R. (2003) Structure and autoregulation of the yeast Hst2 homolog of Sir2. *Nat. Struct. Biol.* **10**, 864–871
  28. Sauve, A. A., and Youn, D. Y. (2012) Sirtuins: NAD(+)-dependent deacetylase mechanism and regulation. *Curr. Opin. Chem. Biol.* **16**, 535–543
  29. Wang, Y., Fung, Y. M. E., Zhang, W., He, B., Chung, M. W. H., Jin, J., et al. (2017) Deacylation mechanism by SIRT2 revealed in the 1'-SH-2'-O-myristoyl intermediate structure. *Cell Chem. Biol.* **24**, 339–345
  30. Teng, Y. B., Jing, H., Aramsangtienchai, P., He, B., Khan, S., Hu, J., et al. (2015) Efficient demyristoylase activity of SIRT2 revealed by kinetic and structural studies. *Sci. Rep.* **5**, 8529
  31. Moniot, S., Schutkowski, M., and Steegborn, C. (2013) Crystal structure analysis of human Sirt2 and its ADP-ribose complex. *J. Struct. Biol.* **182**, 136–143
  32. Feldman, J. L., Dittenhafer-Reed, K. E., Kudo, N., Thelen, J. N., Ito, A., Yoshida, M., et al. (2015) Kinetic and structural basis for acyl-group selectivity and NAD(+) dependence in sirtuin-catalyzed deacylation. *Biochemistry* **54**, 3037–3050
  33. Chen, L. (2019) *Structural and Functional Study of Human SIRT2 and SIRT1*, The University of Hong Kong, Pokfulam, Hong Kong
  34. Weaver, T. M., Washington, M. T., and Freudenthal, B. D. (2022) New insights into DNA polymerase mechanisms provided by time-lapse crystallography. *Curr. Opin. Struct. Biol.* **77**, 102465
  35. Hong, J. Y., Price, I. R., Bai, J. J., and Lin, H. (2019) A glycoconjugated SIRT2 inhibitor with aqueous solubility allows structure-based design of SIRT2 inhibitors. *ACS Chem. Biol.* **14**, 1802–1810
  36. Galleano, I., Schiedel, M., Jung, M., Madsen, A. S., and Olsen, C. A. (2016) A continuous, fluorogenic sirtuin 2 deacetylase assay: substrate screening and inhibitor evaluation. *J. Med. Chem.* **59**, 1021–1031
  37. Hou, D., Yu, T., Lu, X., Hong, J. Y., Yang, M., Zi, Y., et al. (2024) Sirt2 inhibition improves gut epithelial barrier integrity and protects mice from colitis. *Proc. Natl. Acad. Sci. U. S. A.* **121**, e2319833121
  38. Lin, H. (2023) Substrate-selective small-molecule modulators of enzymes: mechanisms and opportunities. *Curr. Opin. Chem. Biol.* **72**, 102231. <https://doi.org/10.1016/j.cbpa.2022.102231>
  39. Roche, K. L., Remiszewski, S., Todd, M. J., Kulp, J. L., Tang, L., Welsh, A. V., et al. (2023) An allosteric inhibitor of sirtuin 2 deacetylase activity exhibits broad-spectrum antiviral activity. *J. Clin. Invest.* **133**, e158978
  40. Roshdy, E., Mustafa, M., Shaltout, A. E., Radwan, M. O., Ibrahim, M. A. A., Soliman, M. E., et al. (2021) Selective SIRT2 inhibitors as promising anticancer therapeutics: an update from 2016 to 2020. *Eur. J. Med. Chem.* **224**, 113709
  41. Penteado, A. B., Hassanie, H., Gomes, R. A., Silva Emery, F. D., and Goulart Trossini, G. H. (2023) Human sirtuin 2 inhibitors, their mechanisms and binding modes. *Future Med. Chem.* **15**, 291–311
  42. Dai, H., Sinclair, D. A., Ellis, J. L., and Steegborn, C. (2018) Sirtuin activators and inhibitors: promises, achievements, and challenges. *Pharmacol. Ther.* **188**, 140–154
  43. Eiden, C. G., Maize, K. M., Finzel, B. C., Lipscomb, J. D., and Aldrich, C. C. (2017) Rational optimization of mechanism-based inhibitors through determination of the microscopic rate constants of inactivation. *J. Am. Chem. Soc.* **139**, 7132–7135
  44. Yamagata, K., Goto, Y., Nishimasu, H., Morimoto, J., Ishitani, R., Dohmae, N., et al. (2014) Structural basis for potent inhibition of SIRT2 deacetylase by a macrocyclic peptide inducing dynamic structural change. *Structure* **22**, 345–352
  45. Hong, J. Y., Jing, H., Price, I. R., Cao, J., Bai, J. J., and Lin, H. (2020) Simultaneous inhibition of SIRT2 deacetylase and defatty-acylase activities via a PROTAC strategy. *ACS Med. Chem. Lett.* **11**, 2305–2311
  46. Moniot, S., Forgione, M., Lucidi, A., Hailu, G. S., Nebbioso, A., Carafa, V., et al. (2017) Development of 1,2,4-oxadiazoles as potent and selective inhibitors of the human deacetylase sirtuin 2: structure-activity relationship, X-ray crystal structure, and anticancer activity. *J. Med. Chem.* **60**, 2344–2360
  47. Yang, L. L., Wang, H. L., Zhong, L., Yuan, C., Liu, S. Y., Yu, Z. J., et al. (2018) X-ray crystal structure guided discovery of new selective, substrate-mimicking sirtuin 2 inhibitors that exhibit activities against non-small cell lung cancer cells. *Eur. J. Med. Chem.* **155**, 806–823
  48. Colcerasa, A., Friedrich, F., Melesina, J., Moser, P., Vogelmann, A., Tzortzoglou, P., et al. (2024) Structure-activity studies of 1,2,4-oxadiazoles for the inhibition of the NAD(+)-Dependent lysine deacetylase sirtuin 2. *J. Med. Chem.* **67**, 10076–10095
  49. Hong, J. Y., Cassel, J., Yang, J., Lin, H., and Weiser, B. P. (2021) High-throughput screening identifies ascorbyl palmitate as a SIRT2 deacetylase and defatty-acylase inhibitor. *ChemMedChem* **16**, 3484–3494
  50. Nielsen, A. L., Rajabi, N., Kudo, N., Lundø, K., Moreno-Yruela, C., Bæk, M., et al. (2021) Mechanism-based inhibitors of SIRT2: structure-activity relationship, X-ray structures, target engagement, regulation of  $\alpha$ -tubulin acetylation and inhibition of breast cancer cell migration. *RSC Chem. Biol.* **2**, 612–626
  51. Schiedel, M., Rumpf, T., Karaman, B., Lehoczky, A., Oláh, J., Gerhardt, S., et al. (2016) Aminothiazoles as potent and selective Sirt2 inhibitors: a structure-activity relationship study. *J. Med. Chem.* **59**, 1599–1612
  52. Rumpf, T., Gerhardt, S., Einsle, O., and Jung, M. (2015) Seeding for sirtuins: microseed matrix seeding to obtain crystals of human Sirt3 and Sirt2 suitable for soaking. *Acta Crystallogr. F Struct. Biol. Commun.* **71**(Pt 12), 1498–1510

53. Rumpf, T., Schiedel, M., Karaman, B., Roessler, C., North, B. J., Lehoczky, A., *et al.* (2015) Selective Sirt2 inhibition by ligand-induced rearrangement of the active site. *Nat. Commun.* **6**, 6263
54. Sundriyal, S., Moniot, S., Mahmud, Z., Yao, S., Di Fruscia, P., Reynolds, C. R., *et al.* (2017) Thienopyrimidinone based sirtuin-2 (SIRT2)-Selective inhibitors bind in the ligand induced selectivity pocket. *J. Med. Chem.* **60**, 1928–1945
55. Mellini, P., Itoh, Y., Tsumoto, H., Li, Y., Suzuki, M., Tokuda, N., *et al.* (2017) Potent mechanism-based sirtuin-2-selective inhibition by an. *Chem. Sci.* **8**, 6400–6408
56. Kudo, N., Ito, A., Arata, M., Nakata, A., and Yoshida, M. (2018) Identification of a novel small molecule that inhibits deacetylase but not defatty-acylase reaction catalysed by SIRT2. *Philos. Trans. R. Soc. Lond. B Biol. Sci.* **373**, 20170070
57. Howitz, K. T., Bitterman, K. J., Cohen, H. Y., Lamming, D. W., Lavu, S., Wood, J. G., *et al.* (2003) Small molecule activators of sirtuins extend *Saccharomyces cerevisiae* lifespan. *Nature* **425**, 191–196
58. You, W., Zheng, W., Weiss, S., Chua, K. F., and Steegborn, C. (2019) Structural basis for the activation and inhibition of Sirtuin 6 by quercetin and its derivatives. *Sci. Rep.* **9**, 19176
59. You, W., and Steegborn, C. (2021) Binding site for activator MDL-801 on SIRT6. *Nat. Chem. Biol.* **17**, 519–521
60. You, W., Rotili, D., Li, T. M., Kambach, C., Meleshin, M., Schutkowski, M., *et al.* (2017) Structural basis of sirtuin 6 activation by synthetic small molecules. *Angew. Chem. Int. Ed. Engl.* **56**, 1007–1011
61. Huang, Z., Zhao, J., Deng, W., Chen, Y., Shang, J., Song, K., *et al.* (2018) Identification of a cellularly active SIRT6 allosteric activator. *Nat. Chem. Biol.* **14**, 1118–1126
62. Klein, M. A., Liu, C., Kuznetsov, V. I., Feltenberger, J. B., Tang, W., and Denu, J. M. (2020) Mechanism of activation for the sirtuin 6 protein deacetylase. *J. Biol. Chem.* **295**, 1385–1399
63. Feldman, J. L., Baeza, J., and Denu, J. M. (2013) Activation of the protein deacetylase SIRT6 by long-chain fatty acids and widespread deacetylation by mammalian sirtuins. *J. Biol. Chem.* **288**, 31350–31356
64. Bi, D., Yang, J., Hong, J. Y., Parikh, P., Hinds, N., Infanti, J., *et al.* (2020) Substrate-dependent modulation of SIRT2 by a fluorescent probe, 1-aminoanthracene. *Biochemistry* **59**, 3869–3878
65. Weiser, B. P., and Eckenhoff, R. G. (2015) Propofol inhibits SIRT2 deacetylase through a conformation-specific, allosteric site. *J. Biol. Chem.* **290**, 8559–8568
66. Head, P. E., Zhang, H., Bastien, A. J., Koyen, A. E., Withers, A. E., Dad-dacha, W. B., *et al.* (2017) Sirtuin 2 mutations in human cancers impair its function in genome maintenance. *J. Biol. Chem.* **292**, 9919–9931
67. Nahhas, F., Dryden, S. C., Abrams, J., and Tainsky, M. A. (2007) Mutations in SIRT2 deacetylase which regulate enzymatic activity but not its interaction with HDAC6 and tubulin. *Mol. Cell Biochem.* **303**, 221–230
68. Inoue, T., Hiratsuka, M., Osaki, M., Yamada, H., Kishimoto, I., Yamaguchi, S., *et al.* (2007) SIRT2, a tubulin deacetylase, acts to block the entry to chromosome condensation in response to mitotic stress. *Oncogene* **26**, 945–957
69. North, B. J., Marshall, B. L., Borra, M. T., Denu, J. M., and Verdin, E. (2003) The human Sir2 ortholog, SIRT2, is an NAD<sup>+</sup>-dependent tubulin deacetylase. *Mol. Cell* **11**, 437–444
70. Seo, K. S., Park, J. H., Heo, J. Y., Jing, K., Han, J., Min, K. N., *et al.* (2015) SIRT2 regulates tumour hypoxia response by promoting HIF-1 $\alpha$  hydroxylation. *Oncogene* **34**, 1354–1362
71. North, B. J., and Verdin, E. (2007) Mitotic regulation of SIRT2 by cyclin-dependent kinase 1-dependent phosphorylation. *J. Biol. Chem.* **282**, 19546–19555
72. Kim, H. S., Vassilopoulos, A., Wang, R. H., Lahusen, T., Xiao, Z., Xu, X., *et al.* (2011) SIRT2 maintains genome integrity and suppresses tumorigenesis through regulating APC/C activity. *Cancer Cell* **20**, 487–499
73. Jing, H., Zhang, X., Wisner, S. A., Chen, X., Spiegelman, N. A., Linder, M. E., *et al.* (2017) SIRT2 and lysine fatty acylation regulate the transforming activity of K-Ras4a. *Elife* **6**, e32436
74. Pandithage, R., Lilischkis, R., Harting, K., Wolf, A., Jedamzik, B., Lüscher-Firzlaff, J., *et al.* (2008) The regulation of SIRT2 function by cyclin-dependent kinases affects cell motility. *J. Cell Biol.* **180**, 915–929
75. Pereira, J. M., Chevalier, C., Chaze, T., Gianetto, Q., Impens, F., Matondo, M., *et al.* (2018) Infection reveals a modification of SIRT2 critical for chromatin association. *Cell Rep.* **23**, 1124–1137
76. Abeywardana, M. Y., Whedon, S. D., Lee, K., Nam, E., Dovarganes, R., DuBois-Coyne, S., *et al.* (2024) Multifaceted regulation of sirtuin 2 (Sirt2) deacetylase activity. *J. Biol. Chem.* **300**, 107722
77. Bohl, K., Wynia-Smith, S. L., Jones Lipinski, R. A., and Smith, B. C. (2024) Inhibition of sirtuin deacetylase activity by peroxyntirite. *Biochemistry* **63**, 2463–2476
78. Kalous, K. S., Wynia-Smith, S. L., and Smith, B. C. (2021) Sirtuin oxidative post-translational modifications. *Front. Physiol.* **12**, 763417
79. Kalous, K. S., Wynia-Smith, S. L., Summers, S. B., and Smith, B. C. (2020) Human sirtuins are differentially sensitive to inhibition by nitrosating agents and other cysteine oxidants. *J. Biol. Chem.* **295**, 8524–8536
80. Han, Y., Jin, Y. H., Kim, Y. J., Kang, B. Y., Choi, H. J., Kim, D. W., *et al.* (2008) Acetylation of Sirt2 by p300 attenuates its deacetylase activity. *Biochem. Biophys. Res. Commun.* **375**, 576–580
81. Black, J. C., Mosley, A., Kitada, T., Washburn, M., and Carey, M. (2008) The SIRT2 deacetylase regulates autoacetylation of p300. *Mol. Cell* **32**, 449–455
82. Gunning, P. W. (2001) Protein isoforms and isozymes. In *Encyclopedia of Life Sciences*. Nature Publishing Group, London, UK
83. Rack, J. G., VanLinden, M. R., Lutter, T., Aasland, R., and Ziegler, M. (2014) Constitutive nuclear localization of an alternatively spliced sirtuin-2 isoform. *J. Mol. Biol.* **426**, 1677–1691
84. Piracha, Z. Z., Saeed, U., Kim, J., Kwon, H., Chwae, Y. J., Lee, H. W., *et al.* (2020) An alternatively spliced sirtuin 2 isoform 5 inhibits hepatitis B virus replication from cccDNA by repressing epigenetic modifications made by histone lysine methyltransferases. *J. Virol.* **94**, e00926-20
85. Lee, Y. G., Reader, B. F., Herman, D., Streicher, A., Englert, J. A., Ziegler, M., *et al.* (2019) Sirtuin 2 enhances allergic asthmatic inflammation. *JCI Insight* **4**, e124710
86. Zhao, K., Chai, X., and Marmorstein, R. (2004) Structure and substrate binding properties of cobB, a Sir2 homolog protein deacetylase from *Escherichia coli*. *J. Mol. Biol.* **337**, 731–741
87. Yang, Y., Ding, J., Gao, Z. G., and Wang, Z. J. (2017) A variant in SIRT2 gene 3'-UTR is associated with susceptibility to colorectal cancer. *Oncotarget* **8**, 41021–41025
88. Zheng, X., Li, J., Sheng, J., Dai, Y., Wang, Y., Liu, J., *et al.* (2020) Haplotypes of the mutated SIRT2 promoter contributing to transcription factor binding and type 2 diabetes susceptibility. *Genes (Basel)* **11**, 569
89. Yang, W., Gao, F., Zhang, P., Pang, S., Cui, Y., Liu, L., *et al.* (2017) Functional genetic variants within the SIRT2 gene promoter in acute myocardial infarction. *PLoS One* **12**, e0176245
90. Song, J., Yang, B., Jia, X., Li, M., Tan, W., Ma, S., *et al.* (2018) Distinctive roles of sirtuins on diabetes, protective or detrimental? *Front. Endocrinol. (Lausanne)* **9**, 724
91. Chen, X., Lu, W., and Wu, D. (2021) Sirtuin 2 (SIRT2): confusing roles in the pathophysiology of neurological disorders. *Front. Neurosci.* **15**, 614107
92. Budayeva, H. G., and Cristea, I. M. (2016) Human sirtuin 2 localization, transient interactions, and impact on the proteome point to its role in intracellular trafficking. *Mol. Cell Proteomics* **15**, 3107–3125
93. Zhu, C., Dong, X., Wang, X., Zheng, Y., Qiu, J., Peng, Y., *et al.* (2022) Multiple roles of SIRT2 in regulating physiological and pathological signal transduction. *Genet. Res. (Camb)* **2022**, 9282484
94. Cao, Z., Yan, Q., Zhang, M., Zhu, Y., Liu, J., Jiang, Y., *et al.* (2022) FHL1 mediates HOXA10 deacetylation via SIRT2 to enhance blastocyst-epithelial adhesion. *Cell Death Discov* **8**, 461
95. Ramakrishnan, G., Davaakhuu, G., Kaplun, L., Chung, W. C., Rana, A., Atfi, A., *et al.* (2014) Sirt2 deacetylase is a novel AKT binding partner critical for AKT activation by insulin. *J. Biol. Chem.* **289**, 6054–6066
96. Hamaidi, I., Zhang, L., Kim, N., Wang, M. H., Iclozan, C., Fang, B., *et al.* (2020) Sirt2 inhibition enhances metabolic fitness and effector functions of tumor-reactive T cells. *Cell Metab.* **32**, 420–436.e412

97. Cha, Y., Han, M. J., Cha, H. J., Zoldan, J., Burkart, A., Jung, J. H., *et al.* (2017) Metabolic control of primed human pluripotent stem cell fate and function by the miR-200c-SIRT2 axis. *Nat. Cell Biol.* **19**, 445–456
98. Knyphausen, P., de Boor, S., Kuhlmann, N., Scislawski, L., Extra, A., Baldus, L., *et al.* (2016) Insights into lysine deacetylation of natively folded substrate proteins by sirtuins. *J. Biol. Chem.* **291**, 14677–14694
99. Chio, U. S., Rechiche, O., Bryll, A. R., Zhu, J., Leith, E. M., Feldman, J. L., *et al.* (2023) Cryo-EM structure of the human Sirtuin 6-nucleosome complex. *Sci. Adv.* **9**, eadf7586
100. Wang, Z. A., Markert, J. W., Whedon, S. D., Yapa Abeywardana, M., Lee, K., Jiang, H., *et al.* (2023) Structural basis of sirtuin 6-catalyzed nucleosome deacetylation. *J. Am. Chem. Soc.* **145**, 6811–6822
101. Hsu, W. W., Wu, B., and Liu, W. R. (2016) Sirtuins 1 and 2 are universal histone deacetylases. *ACS Chem. Biol.* **11**, 792–799
102. Budayeva, H. G., Rowland, E. A., and Cristea, I. M. (2016) Intricate roles of mammalian sirtuins in Defense against viral pathogens. *J. Virol.* **90**, 5–8
103. Koyuncu, E., Budayeva, H. G., Miteva, Y. V., Ricci, D. P., Silhavy, T. J., Shenk, T., *et al.* (2014) Sirtuins are evolutionarily conserved viral restriction factors. *mBio* **5**, e02249-14
104. Pannek, M., Simic, Z., Fuszard, M., Meleshin, M., Rotili, D., Mai, A., *et al.* (2017) Crystal structures of the mitochondrial deacylase Sirtuin 4 reveal isoform-specific acyl recognition and regulation features. *Nat. Commun.* **8**, 1513
105. Kairys, V., Gilson, M. K., Lather, V., Schiffer, C. A., and Fernandes, M. X. (2009) Toward the design of mutation-resistant enzyme inhibitors: further evaluation of the substrate envelope hypothesis. *Chem. Biol. Drug Des.* **74**, 234–245
106. O'Reilly, M., Cleasby, A., Davies, T. G., Hall, R. J., Ludlow, R. F., Murray, C. W., *et al.* (2019) Crystallographic screening using ultra-low-molecular-weight ligands to guide drug design. *Drug Discov. Today* **24**, 1081–1086
107. Schiedel, M., Rumpf, T., Karaman, B., Lehotzky, A., Gerhardt, S., Ovádi, J., *et al.* (2016) Structure-based development of an affinity probe for sirtuin 2. *Angew. Chem. Int. Edition* **55**, 2252–2256